Risk-Sensitive Security-Constrained Economic Dispatch via Critical Region Exploration

Final Project Report

S-88G

Power Systems Engineering Research Center
Empowering Minds to Engineer
the Future Electric Energy System

Risk-Sensitive Security-Constrained Economic Dispatch via Critical Region Exploration

Final Project Report

Project Team
Subhonmesh Bose, Project Leader
University of Illinois at Urbana-Champaign

Graduate Students
Avinash N. Madavan
Mariola Ndrio
University of Illinois at Urbana-Champaign

PSERC Publication 21-11

October 2021

For information about this project, contact:

Subhonmesh Bose
4058 ECE Building
306 N. Wright St.,
Urbana 91801.
Tel: +1-217-244-2101

Power Systems Engineering Research Center

The Power Systems Engineering Research Center (PSERC) is a multi-university Center conducting research on challenges facing the electric power industry and educating the next generation of power engineers. More information about PSERC can be found at the Center's website: http://www.pserc.org.

For additional information, contact:

Power Systems Engineering Research Center
Arizona State University
527 Engineering Research Center
Tempe, Arizona 85287-5706
Phone: 480-965-1643
Fax: 480-727-2052

Notice Concerning Copyright Material

Acknowledgements

We wish to thank our industry advisor Tongxin Zheng (ISO-NE) for supporting this project.

We also thank Ye Guo (Tsinghua-Berkeley-Shenzen Institute), Lang Tong (Cornell) and Hassan Hijazi (Los Alamos National Laboratory) for their contributions on this project.

Executive Summary

Power system operation faces two kinds of uncertainties. The first type relates to failures of system components such as generators and transmission lines. Such events (or contingencies) are rare. However, when they occur, their impact on the power system can be substantial, affecting a large population. The second kind of uncertainty emanates from renewable generation from resources such as wind and solar. Given the aggressive integration of such resources, the supply side is becoming increasingly uncertain. Electricity markets must accommodate their variability in everyday operations. Market design must effectively model these two types of uncertainties, find efficient algorithms to clear the market and find meaningful ways to design settlements for market participants.

Power system often adopts one of two ways to tackle uncertainty. The first among these approaches aims to define plans for the average case prior to the uncertainty being realized. Such an approach leaves the system vulnerable to potentially large operational costs required to handle attending deviations in real-time. On the other extreme, the second approach aims to plan for the worst-case scenario. This robust approach to forward planning is overly conservative and prioritizes reliability at the expense of possibly large operational costs. This PSERC project advocates for an in-between—the risk-sensitive approach to electricity market design under uncertainty. Risk defines an attitude towards uncertain outcomes. Suitably defined risk measures can effectively explore the cost-reliability tradeoff.

With roots in mathematical finance, risk measures abound in the literature. Some measures are more amenable to algorithm and pricing design than others. The works presented in this final report leverages the conditional-value-at-risk (CVaR) measure. CVaR-based market clearing formulations with both kinds of uncertainties and linearized power flow models become convex optimization problems. It is this convexity that makes algorithm and pricing design easy. With contingencies, the market clearing problem becomes a large linear program that can be efficiently decomposed, and its computation can be parallelized. With renewable generation, the CVaR-based market clearing problem can be solved with wind data. The mature duality theory of convex programming allows derivation of meaningful prices from these convex optimization-based market clearing formulations.

Concretely, this final report collects three lines of work, described below.

A. Risk-Sensitive Security-Constrained Economic Dispatch (SCED): This work considers uncertainty in transmission line failures and proposes a risk-sensitive security-constrained market clearing formulation that allows an SO to tradeoff between cost of nominal dispatch and the extent of possible load-shedding. The formulation provides a tunable parameter that allows the SO to systematically explore this tradeoff. The CVaR-based optimization problem for market clearing is then solved via an algorithm that leverages the problem structure. More precisely, the optimization problem is a large linear program where the corrective action in each contingency is only coupled to the nominal dispatch and not the actions in other contingencies. This nature of coupling allows a decomposition of the problem that permits parallelization. The work in this area has largely revolved around finding suitable ways to exploit the problem structure to design a fast algorithm.

B. Risk-Sensitive Economic Dispatch with Random Wind: This work proposes a framework to compute a risk-sensitive dispatch that defines a forward dispatch against uncertain wind power production. Wind renders power draws from generation assets and power flows over the transmission lines uncertain. The proposed market-clearing formulation penalizes constraint violations and random costs via their conditional value at risks (CVaRs). This formulation with linear power flow equations is a convex optimization problem. A data-driven solution architecture is proposed to solve the problem. This algorithm generates uncertain wind scenarios across the network and moves the solution iterates accordingly. The mathematical analysis reveals how increased risk aversion leads to higher sample complexity, and hence, longer solution time.

C. Pricing Risk-Sensitive Economic Dispatch with Wind. This work defines prices from the risk-sensitive market clearing formulation that guards against uncertain wind. These prices depend on the assets connected to the network, their uncertainties in power injections and the risk attitudes in dealing with said uncertainties. Properties of these risk-sensitive locational marginal prices (risk-LMPs) are derived using duality theory of convex programming. Specifically, these prices are shown to be the risk-sensitive extensions to traditional LMPs in that zeroing out the wind variance reduces these prices to traditional LMPs. They are shown to equal the sensitivity of the optimal cost of the risk-sensitive economic dispatch problem to nodal demands. Sufficient conditions are derived for revenue adequacy to be non-negative. A data-driven algorithm using wind scenarios is designed to approximate these prices.

Project Publications:

[1] A. N. Madavan, S. Bose, Y. Guo and L. Tong, "Risk-Sensitive Security-Constrained Economic Dispatch via Critical Region Exploration", Proceedings of the IEEE Power and Energy Society General Meeting, 2019.

[2] A. N. Madavan, and S. Bose, "Risk-Sensitive Energy Procurement with Uncertain Wind", Proceedings of the IEEE Global Conference on Signal and Information Processing (GlobalSIP), 2019.

[3] A. N. Madavan and S. Bose, "A Stochastic Primal-Dual Method for Optimization with Conditional Value at Risk Constraints", Accepted in the Journal of Optimization Theory and Applications, 2021.

[4] M. Ndrio, A. N. Madavan and S. Bose, "Pricing Conditional Value at Risk-Sensitive Economic Dispatch", Accepted for presentation at the IEEE Power and Energy Society General Meeting, 2021.

Student Theses:

[1] A. N. Madavan, "Risk-Sensitive Optimization for Power Systems". Ph.D. thesis. University of Illinois at Urbana-Champaign. (Expected) June 2022.

[2] M. Ndrio, "Equilibrium and Learning in Electricity Markets: A Scalar-Parameterized Supply and Demand Function Approach". Ph.D. thesis. University of Illinois at Urbana-Champaign. January 2021.

Table of Contents

List of Figures

List of Tables

1. Introduction

In this final report for the PSERC project S-88G, we present a collection of published papers as chapters that focus on defining risk-sensitive market clearing. Mathematically, risk models the attitude of a decision-maker towards random outcomes. In this project, we consider randomness in renewable generation and component failure scenarios. The goal is a market clearing formulation that allows efficient algorithm and pricing design.

- Chapter 2 considers a risk-sensitive security-constrained economic dispatch (R-SCED) problem that permits a system operator to systematically tradeoff between the cost of power procurement and the reliability of power delivery in the event of a component failure. The formulation considers the uncertainty in failure scenarios through the conditional value at risk (CVaR) measure. The formulation results in a large linear program, that is solved via the critical region exploration (CRE) algorithm. This algorithm takes advantage of the structure of the constraints to permit decomposition for efficient solution.

- Chapter 3 considers a risk-sensitive forward energy procurement problem with uncertain wind. This formulation penalizes costs and constraint violations via the conditional value at risk (CVaR) measure. This market clearing formulation allows a system operator to reflect their tolerance to high uncertain costs and constraint violations. The problem is solved via a stochastic primal-dual algorithm.

- Chapter 4 considers a market clearing problem very similar to that in Chapter 3, but proposes risk-sensitive locational marginal prices (risk-LMPs) to accompany such a dispatch. Risk-LMPs extend conventional LMPs to the uncertain setting. Settlements defined via risk-LMPs compensate resources for both energy and regulation. These prices are computed via sample average approximation with wind samples.

2. Risk-Sensitive Security-Constrained Economic Dispatch

2.1 Introduction

System operators (SOs) routinely solve a security-constrained economic dispatch (SCED) problem to compute dispatch decisions to meet demand requirements over a transmission network. SOs often seek a dispatch that is robust to all single potential outages of transmission lines, transformers, or generators, to maintain the so-called $N-1$ *security criterion* for an N-component power system.

SCED tries to balance between the SO's two conflicting goals – minimizing power procurement costs and maintaining reliability of power delivery under a collection of counterfactual scenarios called contingencies. Most formulations in the literature sacrifice cost considerations to prioritize reliability. In this work, we propose a risk-sensitive SCED (R-SCED) problem that provides the SO a tunable parameter to tradeoff between cost and reliability. We also provide a computational procedure to solve R-SCED under linearized power flow models.

SCED formulations abound in the literature; the first of which is *preventive*-SCED (P-SCED). This formulation enforces that the nominal dispatch remains feasible within existing limits for all operational components in every contingency [1]. P-SCED does not consider potential recourse actions following a contingency and the resulting dispatch is overly conservative. *Corrective*-SCED (C-SCED) expands upon P-SCED by allowing active network components to respond to a contingency, e.g., see [2]. It allows re-dispatch of generators with fast-ramping capabilities and some even allow partial load-shedding, e.g., see [3–5]. Most C-SCED formulations ignore costs associated with recourse actions. Such costs can be high, especially for potential load shedding modeled via *value of lost load*. To remedy that, authors in [6] associate probabilities to contingencies and advocate to minimize the expected dispatch costs across contingencies. In contrast, our R-SCED formulation in Section 2.2 proposes to minimize the *conditional value at risk* (CVaR) of said costs. CVaR_α of a random variable measures the expected loss in the $1-\alpha$ fraction of the worst outcomes. In Section 2.3, we explore the properties of R-SCED and illustrate through a two-bus network example, how the SO can express its preference in trading off cost versus reliability through its choice of α in R-SCED.

The R-SCED problem has a much larger problem description compared to a nominal economic dispatch problem owing to the number of contingencies, which leads to computational difficulties that are shared by other C-SCED formulations. To deal with this challenge, many have suggested to pre-filter contingencies; see [7] for a survey. In this work, we consider a decomposition approach to divide the R-SCED problem into smaller subproblems that can potentially be solved in parallel. We propose a critical region exploration (CRE) algorithm in Section 2.4 to solve the R-SCED problem. CRE leverages properties of multiparametric linear programming and has proven effective in the tie-line scheduling problem for multi-area power systems in [8]. We demonstrate the efficacy of our algorithm on the IEEE 30-bus test system in Section 2.5. This chapter is based on the work in [9]; proofs of all claims can be found there and are omitted from here for brevity.

2.2 Risk-sensitive SCED problem

We formulate the risk-sensitive SCED (R-SCED) problem with the linear DC power flow model and discuss how it generalizes prior formulations. R-SCED can easily be extended to more detailed nonlinear AC power flow equations. In practice, however, SOs often solve a sequence of SCED problems with successive linearizations of power flow equations to handle nonlinearity [10].

2.2.1 Network model

We begin by describing our model for the power network. Consider a grid on n buses, labeled $1,\ldots,n$, with m transmission lines. Let each bus be equipped with a dispatchable generator and a nominal load, whose vector values are denoted $\boldsymbol{g} \in \mathbb{R}^n$ and $\overline{\boldsymbol{d}} \in \mathbb{R}^n$, respectively. We adopt a linear power flow model via DC approximations, where the (directed) power flows over the transmission lines are linear maps of the vector of nodal power injections $\boldsymbol{x}$, given by $\boldsymbol{H}\boldsymbol{x}$. Here, $\boldsymbol{H} \in \mathbb{R}^{2m\times n}$ denotes the injection shift-factor matrix that depends on the topology of the power network and the admittances of the transmission lines. Let the limits on the (directed) power flows be denoted by $\boldsymbol{f} \in \mathbb{R}^{2m}$. The set of allowable nodal power injections then becomes

$$\mathbb{P} := \{\boldsymbol{x} \in \mathbb{R}^n \mid \boldsymbol{H}\boldsymbol{x} \leq \boldsymbol{f},\ \mathbb{1}^\intercal \boldsymbol{x} = 0\}, \tag{2.1}$$

where $\mathbb{1} \in \mathbb{R}^n$ is a vector of all ones. The equality $\mathbb{1}^\intercal \boldsymbol{x} = 0$ captures the balance of demand and supply of power across the network. The DC approximations deem the voltage magnitudes to be at their nominal values, ignore transmission line losses, and assume that voltage phase angle differences across neighboring buses are small.[1] Assume that a linear dispatch cost $\boldsymbol{c}^\intercal \boldsymbol{g}$ to produce $\boldsymbol{g}$ from the dispatchable generators can vary their outputs within $\mathbb{G} = [\underline{\boldsymbol{G}}, \overline{\boldsymbol{G}}]$. The lack of a generator at bus i can be modeled by letting $\underline{G}_i = \overline{G}_i = 0$.

2.2.2 Modeling contingencies

Consider a collection of scenarios, denoted by $1,\ldots,K$, each of which corresponds to a single transmission line failure. In the event of a contingency, we allow the operator to take recourse actions; they may alter generator output within ramping capabilities and shed load. Let $\delta\boldsymbol{g}^k$ denote the deviation of supply from the generators in contingency k from the nominal case, constrained by ramping limitations modeled as $|\delta\boldsymbol{g}^k| \leq \boldsymbol{\Delta}_g$. Denote the amount of load shed by $\delta\boldsymbol{d}^k \in [0, \overline{\boldsymbol{d}} - \underline{\boldsymbol{d}}] := \boldsymbol{\Delta}_d$ in contingency k.

A line outage alters the network topology, and hence, results in a different injection shift factor matrix $\boldsymbol{H}^k$ that in turn defines a different feasible injection region $\mathbb{P}^k$. Transfer capabilities of transmission lines are primarily determined by thermal considerations, and can exceed their rated power capacities for short durations. Following [12] and prior formulations [3, 5, 13], we adopt relaxed line ratings under contingencies. The *drastic action* limits are adopted immediately follow-

[1] We can alternatively utilize linearization of the power flow equations around the current operating point, possibly using real-time measurements to estimate $\boldsymbol{H}$, e.g., in [11].

ing a contingency, but before recourse actions are taken, and the *short-term emergency* limits are adopted after a short time (e.g., 5 minutes) from when the SO takes the recourse actions. Let the corresponding sets of feasible injections be denoted $\mathbb{P}^k_{\mathsf{DA}}$ and $\mathbb{P}^k_{\mathsf{SE}}$ respectively, where

$$\mathbb{P}^k \subset \mathbb{P}^k_{\mathsf{SE}} \subset \mathbb{P}^k_{\mathsf{DA}}.$$

2.2.3 Formulating the risk-sensitive SCED (R-SCED) problem

Our formulation relies on the use of *conditional value at risk* of a random variable. We begin by describing this risk measure and then present R-SCED in (2.2).

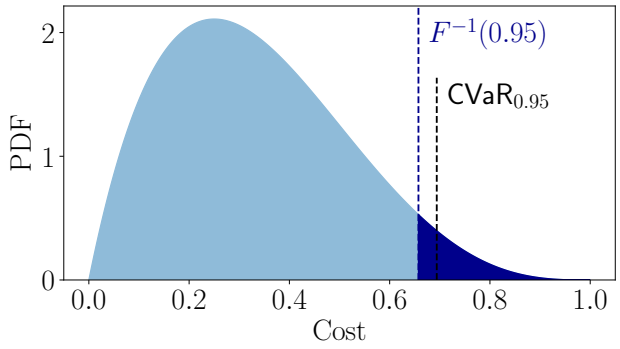

Figure 2.1: The probability distribution of random cost with the shaded region denoting the tail of the distribution with probability 0.05.

If χ describes a random cost with a continuous distribution, $\mathrm{CVaR}_\alpha[\chi]$ computes the expected cost of χ in the $(1-\alpha)$ fraction of worst-case outcomes, or

$$\mathrm{CVaR}_\alpha[\chi] := \mathbb{E}\left[\chi | \chi \geq F^{-1}(\alpha)\right],$$

where F is the cumulative distribution function of χ and $\mathbb{E}$ denotes the expectation computed over that distribution. Figure 2.1 visualizes the definition for some probability distribution of random cost χ. $\mathrm{CVaR}_{0.95}[\chi]$ is the average value of χ over the distribution of shaded tail where the tail has probability 0.05. As $\alpha \downarrow 0$, $\mathrm{CVaR}_\alpha[\chi]$ reduces to the expected value of χ. For α close to 1, the tail shrinks to only include the maximum value of χ and $\mathrm{CVaR}_\alpha[\chi]$ yields that maximum.[2]

To present R-SCED formally, associate probabilities $\boldsymbol{p} \in \mathbb{R}^K$ to the contingencies and let $p_0 := 1 - \mathbb{1}^\intercal \boldsymbol{p}$ as the probability of the nominal state. We arrive at the following optimization problem of

[2] For the definition of $\mathrm{CVaR}_\alpha[\chi]$ for χ with general distributions, see [14].

the *risk-sensitive* SCED problem.

$$\begin{aligned}
\text{minimize}\quad & \mathrm{CVaR}_{\alpha}\left[\boldsymbol{c}^{\mathsf{T}}\boldsymbol{g}+C(\delta\boldsymbol{g},\delta\boldsymbol{d})\right], && \text{(2.2a)}\\
\text{subject to}\quad & \boldsymbol{g}\in\mathbb{G},\ \boldsymbol{g}-\overline{\boldsymbol{d}}\in\mathbb{P},\boldsymbol{g}-\overline{\boldsymbol{d}}\in\mathbb{P}^{k}_{\mathsf{DA}}, && \text{(2.2b)}\\
& \boldsymbol{g}+\delta\boldsymbol{g}^{k}\in\mathbb{G},\boldsymbol{g}+\delta\boldsymbol{g}^{\boldsymbol{k}}-\overline{\boldsymbol{d}}+\delta\boldsymbol{d}^{k}\in\mathbb{P}^{k}_{\mathsf{SE}}, && \text{(2.2c)}\\
& |\delta\boldsymbol{g}^{k}|\leq\boldsymbol{\Delta}_{g},\ \delta\boldsymbol{d}^{k}\in\boldsymbol{\Delta}_{d}, && \text{(2.2d)}\\
& \text{for each } k=1,\ldots,K
\end{aligned}$$

over $\boldsymbol{g}$, $\delta\boldsymbol{g}$, $\delta\boldsymbol{d}$. Here, $\delta\boldsymbol{g}$, $\delta\boldsymbol{d}$ denote the collection of the respective variables across all contingencies. Additionally, $C(\delta\boldsymbol{g},\delta\boldsymbol{d})$ is the random recourse cost, assuming a contingency occurs, that takes the value

$$C^{k}(\delta\boldsymbol{g}^{k},\delta\boldsymbol{d}^{k}):=\boldsymbol{c}^{\mathsf{T}}\delta\boldsymbol{g}^{k}+\boldsymbol{v}^{\mathsf{T}}\delta\boldsymbol{d}^{k}$$

in contingency k.[3] Here, $\boldsymbol{v}$ measures the vector of nodal values of lost load (VoLL).

In R-SCED , the dispatch cost depends on two factors — the dispatch decisions and the realized contingency. Fixing the decisions, the cost is a random variable over the set of contingencies. Minimizing the expected value of this random variable yields the formulation in [6]. Taking the CVaRof this variable generalizes this to encode an SO's tolerance to higher costs through the parameter α. Choosing α equal to zero, R-SCED treats all contingencies equally and minimizes expected cost as in [6]. As α increases, R-SCED weighs contingencies where the cost is higher more heavily.

For convenience, we denote the dispatch associated with nominal operation, $\boldsymbol{g}$, as *nominal dispatch* and the associated cost, $\boldsymbol{c}^{\mathsf{T}}\boldsymbol{g}$, as *nominal dispatch cost*.

2.2.4 Comparison to existing SCED formulations

Before delineating the properties of the R-SCED problem in the next section, we briefly discuss its relationship to prior formulations of the SCED problem in the literature. We refer the reader to [5] for a comprehensive survey.

- Preventive SCED (P-SCED) stipulates that the nominal dispatch be feasible after any single line failure, and does not model recourse actions or temporarily relaxed line ratings. R-SCED with $\Delta_g=\Delta_d=0$ and $\mathbb{P}^{k}_{\mathsf{DA}}=\mathbb{P}^{k}_{\mathsf{SE}}=\mathbb{P}^{k}$ reduces to P-SCED.

- Corrective SCED (C-SCED) often does not model recourse costs or load shedding. When they are, e.g., in [6], expected costs are minimized—the case of R-SCED with $\alpha=0$.

[3] The cost structure can be altered to distinguish between different costs for regulation up and down, i.e., by replacing $\boldsymbol{c}^{\mathsf{T}}\delta\boldsymbol{g}^{k}$ in the recourse cost by $\boldsymbol{c}_{+}^{\mathsf{T}}[\delta\boldsymbol{g}^{k}]^{+}+\boldsymbol{c}_{-}^{\mathsf{T}}[-\delta\boldsymbol{g}^{k}]^{+}$ without adding conceptual difficulties.

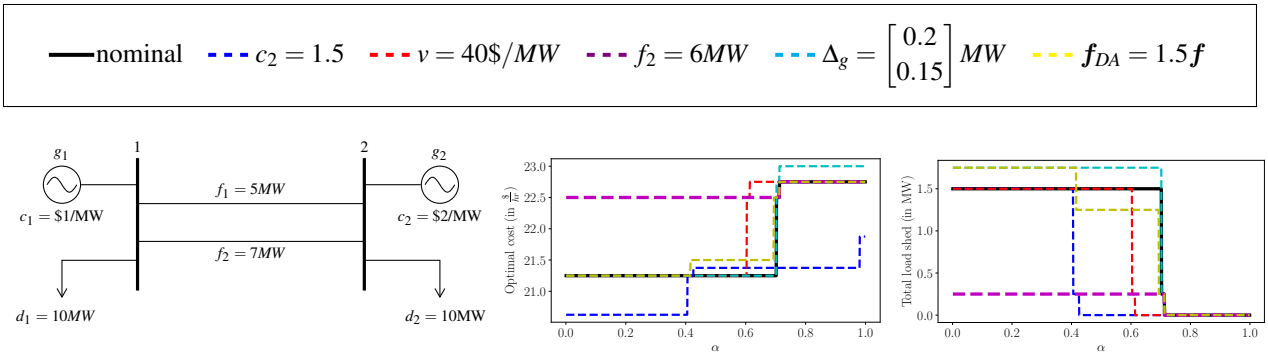

(a) A two-bus network (b) Optimal dispatch cost (c) Total load shedding

Figure 2.2: Nominal cost and total load shedding from either contingency for 2-bus example in (a) is depicted for various parameter choices.

2.3 Properties of the R-SCED problem

In this section, we first characterize a property of R-SCED in our first result that proves useful in devising an algorithm to solve it in Section 2.4. Second, we discuss the outcome of R-SCED on a two-bus network example and compare it to that of C-SCED and P-SCED.

Proposition 1. *R-SCED can be formulated as a linear program, linearly parameterized in* α*. Additionally, the optimal cost of R-SCED in* (2.2) *is piecewise affine in* $\alpha' := (1-\alpha)^{-1}$ *over any closed interval in* $\mathbb{R}_+$*, and the optimal nominal dispatch* $\boldsymbol{g}^*$ *remains constant over sub-intervals where the optimal cost is affine.*

R-SCED can be cast as a linear program of the form

$$\begin{aligned} \underset{\boldsymbol{x}^0,\boldsymbol{x}^1,\ldots,\boldsymbol{x}^K}{\text{minimize}} \quad & [\boldsymbol{c}^0]^\mathsf{T}\boldsymbol{x}^0 + \alpha' \sum_{k=1}^{K} \left[\boldsymbol{c}^k\right]^\mathsf{T} \boldsymbol{x}^k, \\ \text{subject to} \quad & \boldsymbol{A}\boldsymbol{x}^0 \leq \boldsymbol{b}, \\ & \boldsymbol{A}^k\boldsymbol{x}^0 + \boldsymbol{E}^k\boldsymbol{x}^k \leq \boldsymbol{b}^k, \\ & k = 1,\ldots,K, \end{aligned} \tag{2.3}$$

with a decomposable structure, a property we leverage to design our algorithm in Section 2.4.

2.3.1 R-SCED on a two-bus network example

To gain insights into the properties of R-SCED, we present a simple yet illustrative two-bus network example and contrast the results of R-SCED with that of P-SCED and C-SCED.

Consider the network in Figure 2.2a with $\Delta_{g_1} = 0.25$ MW/min, $\Delta_{g_2} = 0.2$ MW/min, and $v_1 = v_2 =$ \$30/MW. Assume line failures occur with probabilities $p_1 = p_2 = 0.01$ and dynamic line ratings of $\boldsymbol{f}_{DA} = 1.75\boldsymbol{f}$ and $\boldsymbol{f}_{SE} = 1.25\boldsymbol{f}$. The following table captures the nominal dispatch cost under

various formulations of economic dispatch, where the nominal case is denoted ED.

Method	g_1^* (MW/hr)	g_2^* (MW/hr)	Nominal Cost ($/hr)
ED	20.0	0.0	20.0
P-SCED	15.0	5.0	25.0
C-SCED	17.25	2.75	22.75
C-SCED$_{\text{aug}}$	18.75	1.25	21.25
R-SCED (0.1)	18.75	1.25	21.25
R-SCED (0.9)	17.25	2.75	22.75

Table 2.1: Comparison of various ED formulations.

C-SCED$_{\text{aug}}$ in Table 2.1 is C-SCED augmented with load shedding, where an SO aims to minimize expected cost with recourse. When α is small ($\alpha \approx 0$), the R-SCED solution equals that in the augmented C-SCED solution. Additionally for large α, i.e., $\alpha \approx 1$, R-SCED reduces to expected cost minimization without load shed. For general power networks, the R-SCED solution with $\alpha \approx 1$ is not equal to the C-SCED solution; it minimizes the maximum recourse cost across contingencies balancing the cost associated with load shedding and generator re-dispatch.

Figure 2.1 demonstrates that nominal cost and total load shed are piecewise constant in α. Additionally, as α increases, the cost of nominal dispatch increases while load shedding decreases. This illustrates how SO can utilize α to trade-off between between cost and reliability.

We draw attention to the case when the dispatch cost of the expensive generator at bus 2 is reduced from \$2/MW to \$1.5/MW. For a range of α (approximately 0.6-0.7), the nominal dispatch cost with the reduced c_2 is higher than that with the larger c_2. Reduction in c_2 makes the VoLL relatively larger compared to ramping costs. As a result, R-SCED favors lesser load shedding at lower α's, leading to the behavior depicted in Figure 2.2b and 2.2c.

2.4 Solving R-SCED via critical region exploration

The R-SCED problem in (2.2) can be cast as a linear program (LP). For practical power networks, that LP can be prohibitively large, a property shared by prior C-SCED formulations. We exploit the structure in its reformulation (2.3) and propose the *critical region exploration* algorithm to solve R-SCED. Our algorithm decomposes the problem into a master problem and a collection of subproblems that can be solved in parallel, and leverages properties of multi-parametric linear programming [8]. To describe the algorithm, begin by noticing that (2.3) can be written as

$$\begin{aligned} \underset{\boldsymbol{x}^0}{\text{minimize}} \quad & \left[\boldsymbol{c}^0\right]^{\mathsf{T}} \boldsymbol{x}^0 + \alpha' \sum_{k=1}^{K} J_*^k\left(\boldsymbol{x}^0\right), \\ \text{subject to} \quad & \boldsymbol{A}\boldsymbol{x}^0 \leq \boldsymbol{b}, \end{aligned} \tag{2.4}$$

where

$$\begin{aligned} J_*^k\left(\boldsymbol{x}^0\right) \coloneqq \underset{\boldsymbol{x}^k}{\text{minimize}} \quad & \left[\boldsymbol{c}^k\right]^{\mathsf{T}} \boldsymbol{x}^k, \\ \text{subject to} \quad & \boldsymbol{A}^k \boldsymbol{x}^0 + \boldsymbol{E}^k \boldsymbol{x}^k \leq \boldsymbol{b}^k. \end{aligned} \tag{2.5}$$

Properties of J_*^k are crucial to describe our algorithm. We need additional notation to describe them. Define

$$\mathbb{X}^0 \coloneqq \{\boldsymbol{x} \mid \boldsymbol{A}\boldsymbol{x} \leq \boldsymbol{b}\}.$$

Assume throughout that (2.5) is feasible for any $\boldsymbol{x}^0 \in \mathbb{X}^0$. We say a collection of polyhedral sets $\mathbb{S}_1, \ldots, \mathbb{S}_L$ define a *polyhedral partition* of $\mathbb{S}$, if these L sets are polyhedral, their union spans $\mathbb{S}$, and any intersections are only at their boundaries. Given this definition, we record a vital property of J_*^k in the following lemma.

Lemma 1. *$J_*^k\left(\boldsymbol{x}^0\right)$ is piecewise affine over $\mathbb{X}^0$ and the sets over which it is affine describe a polyhedral partition of $\mathbb{X}^0$.*

Problem (2.5) is a multi-parametric linear program, linearly parameterized by $\boldsymbol{x}^0$. As a consequence, the above claim follows directly from [15, Theorem 7.2]. Hereafter, call the sets in the polyhedral partition as *critical regions*. For a given $\boldsymbol{x}^0 \in \mathbb{X}^0$, one can compute the critical region $\mathbb{C}^k$ that contains $\boldsymbol{x}^0 \in \mathbb{X}^0$ and the affine description of the optimal cost J_*^k over $\mathbb{C}^k$ for each $k = 1, \ldots, K$.[4] More precisely, let the affine description of J_*^k be given by $\left[\boldsymbol{\rho}^k\right]^{\mathsf{T}} \boldsymbol{x}^0 + \eta^k$ over $\mathbb{C}^k$. With the affine descriptions of $J_*^1, \ldots, J_*^K$, we can then solve

$$\begin{aligned} \underset{\boldsymbol{x}^0}{\text{minimize}} \quad & \left[\boldsymbol{c}^0\right]^{\mathsf{T}} \boldsymbol{x}^0 + \alpha' \sum_{k=1}^{K} \left[\boldsymbol{\rho}^k\right]^{\mathsf{T}} \boldsymbol{x}^0 + \alpha' \eta^k, \\ \text{subject to} \quad & \boldsymbol{A}\boldsymbol{x}^0 \leq \boldsymbol{b},\ \boldsymbol{x}^0 \in \cap_{k=1}^{K} \mathbb{C}_k, \end{aligned} \tag{2.6}$$

i.e., (2.4) with the additional constraint $\boldsymbol{x}^0 \in \cap_{k=1}^{K} \mathbb{C}_k$, over which the affine description of J_*^k holds. The above problem can be solved as an LP. We assume that one can determine the *lexicographically smallest* minimizer of (2.6). This provides a tie-breaking rule in the case the minimizer is not unique. The final consideration is a necessary and sufficient condition for $\boldsymbol{x}^{0,*}$ to be a minimizer of (2.4). To that end, $\boldsymbol{x}^{0,*}$ is a minimizer for (2.4) if and only if

$$0 \in \delta J^*\left(\boldsymbol{x}^{0,*}\right) + N_{\mathbb{X}^0}\left(\boldsymbol{x}^{0,*}\right), \tag{2.7}$$

where $\delta J^*(\cdot)$ denotes the sub-differential set of the objective function of (2.4) and $N_{\mathbb{X}^0}$ is the normal cone of $\mathbb{X}^0$. Algorithm 1 presents the CRE algorithm to solve (2.3). The crucial property of our algorithm is summarized next.

[4] We omit the details of the procedure to determine the critical regions and the associated affine cost description due to space limitations.

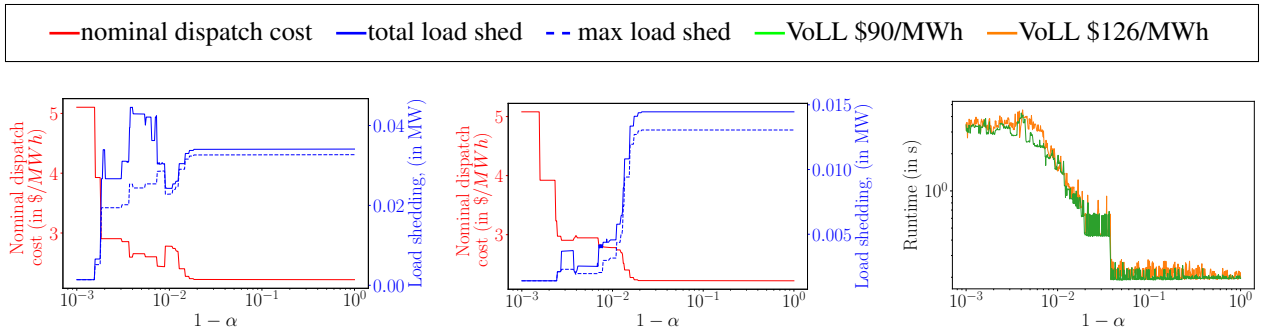

Figure 2.3: R-SCED solutions as a function of α for the IEEE 30-bus test network with VoLL (a) \$90/MWh and (b) \$126/MWh. (c) records the runtime for CRE.

Proposition 2. *Algorithm 1 converges to an optimizer of* (2.3) *in finitely many iterations.*

The proof is largely similar to that of [8, Theorem 1]. See [8,9] for details.

Algorithm 1 CRE algorithm to solve R-SCED.

Initialize:
  $\boldsymbol{x}^0 \in \mathbb{X}^0, J^* \leftarrow \infty, \mathbb{D} \leftarrow$ empty set, $\varepsilon \leftarrow$ small positive number
do
  Given $\boldsymbol{x}^0$, compute $\boldsymbol{\rho}^k, \eta^k, \mathbb{C}^k$ for $k = 1, \ldots, K$.
  Solve (2.6)
  $\left[\boldsymbol{x}^0\right]^{\text{opt}} \leftarrow$ lexicographically smallest minimizer of step 4.
  $J^{\text{opt}} \leftarrow$ optimal cost of step 4
  if $J^{\text{opt}} < J^*$ **then**
    $\left[\boldsymbol{x}^0\right]^* \leftarrow \left[\boldsymbol{x}^0\right]^{\text{opt}}, J^* \leftarrow J^{\text{opt}}, \mathbb{D} \leftarrow \{\boldsymbol{c}\}$
  else
    $\mathbb{D} \leftarrow \mathbb{D} \cup \{\boldsymbol{c}^0 + \alpha' \sum_{k=1}^{K} \boldsymbol{\rho}^k\}$
  end if
  $\boldsymbol{v}^* \leftarrow \operatorname{argmin}_{\boldsymbol{v} \in \operatorname{conv}(\mathbb{D}) + N_{\mathbb{X}^0}\left(\left[\boldsymbol{x}^0\right]^*\right)} \|\boldsymbol{v}\|^2$
  $\boldsymbol{x}^0 \leftarrow \left[\boldsymbol{x}^0\right]^{\text{opt}} - \varepsilon \boldsymbol{v}^*$
while $v^* \neq 0$

2.5 Experiments on the IEEE 30-bus test system

We have implemented CRE for R-SCED on various IEEE test networks. We only report the results on the highly-loaded IEEE 30-bus system from PGLIB v17.08 [16] for space constraints. In our experiments, we assumed drastic action and short-term emergency limits to be 70% and 10% higher than the nominal limits, respectively. Ramping costs were set equal to nominal dispatch costs and ramp limits were uniformly set to 0.2 MW per minute. The system was augmented with generation

capacities of 3MW at buses 13, 22, 23, and 27, and costs were set to \$1.4, 1.8, 1.6, 1.7 per MWh, respectively. Line limits were modified according to Table 2.2.

Bus 1	Bus 2	Line Limit
12	16	0.33
14	15	0.396
16	17	0.36
15	18	0.319
10	20	0.312

Table 2.2: Augmented line limits for IEEE 30-bus example.

Slack variables were added to each subproblem constraint to ensure feasibility, emulating [13]. The algorithm was initialized with the solution of the ED problem with drastic action limits. We formulated the problems in Python, but the CRE algorithm runs on C++. All LPs were solved using Gurobi 8.0. The reported running times are from solutions on a 2015 MacBook Pro with 2.7 GHz Core i5 processor and 8 GB RAM.

As one expects from Proposition 1, Figure 2.3a illustrates that both nominal dispatch cost and load shedding are piecewise constant. While nominal dispatch cost generally increases with risk-aversion, and maximum load shed generally decreases, this does not occur monotonically. This results from the balance of cost associated with load shedding and regulation. When the relative weight of load shedding is increased in Figure 2.3b, R-SCED is less willing to shed load and shows fewer increases in load shed as risk aversion increases.

Additionally, notice the large increase in total load shed despite the maximum load shed not increasing significantly in Figure 2.3a. CVaRconsiders the tail cost of most expensive contingencies and ignores contingencies whose cost is below the cutoff, allowing for a low level of load-shedding throughout each of the contingencies.

3. Risk-Sensitive Energy Procurement with Uncertain Wind

3.1 Introduction

System operators (SOs) procure power to meet demand requirements at various timescales. The forward power procurement process occurs prior to the time of power delivery. Naturally, SOs rely on forecasts of demand/supply conditions to compute such a dispatch. The errors in such forecasts are growing with the aggressive integration of variable renewable energy and distributed energy resources. SOs must therefore explicitly account for the impending uncertainty in demand/supply in the forward power procurement problem. In the sequel, assume that wind power output is the only source of uncertainty. Denote the collective wind power output by $\omega \in \Omega$.

Associated with the dispatch decisions (call it x) are uncertain costs that depend on ω. Call this cost $f_\omega(x)$. Denote the collection of constraints associated with x as

$$g_\omega(x) := (g^1_\omega(x), \ldots, g^p_\omega(x)) \leq 0.$$

These constraints can encode limitations on generation outputs, line limits, etc. With costs and constraint descriptions that depend on the uncertain wind power output, one can adopt a variety of paradigms to define a forward power procurement problem. For example, one can choose to enforce constraints on average and model it as $\mathbb{E}[g^i_\omega(x)] \leq 0$, where the expectation (denoted by $\mathbb{E}$) is computed with respect to a probability distribution $\mathbb{P}$ defined on Ω. Such a constraint enforcement can result in possible constraint violations over a large range of wind power output. In addition, the extent of possible constraint violations can be large as well. An alternate paradigm is to consider a robust constraint enforcement, i.e., to require $g^i_\omega(x) \leq 0$ almost surely for $\omega \in \Omega$. The robust formulation guarantees that constraints will not be violated. However, such formulations can often be overly conservative as one seeks to guard the dispatch decisions against highly improbable yet possible wind power output scenarios. Such stringent constraint enforcement can potentially render the energy procurement problem infeasible.

Uncertain power procurement costs present a similar modeling dilemma. SOs may choose to minimize the average procurement costs, i.e., minimize $\mathbb{E}[f_\omega(x)]$, leaving the system vulnerable to large uncertain costs. They can also choose to minimize the maximum possible procurement cost, an overly conservative modeling paradigm.

In this chapter, we present a risk-sensitive forward power procurement problem formulation with conditional value at risk (CVaR) based penalty on cost and constraint violation. CVaR is a convex risk measure, extensively studied by Rockafellar and Uryasev primarily for applications to risk-sensitive analysis in financial markets [14]. $\text{CVaR}_\beta[g^i_\omega(x)]$ evaluated with the risk parameter β equals the expected value of $g^i_\omega(x)$ over $1-\beta$ fraction of the scenarios with the largest values of $g^i_\omega(x)$. By regulating β, the SO can thus express a tolerance towards possible constraint violation. In particular, for $\beta = 0$, this constraint becomes the same as requiring $\mathbb{E}[g^i_\omega(x)] \leq 0$ and $\beta \uparrow 1$ amounts to a robust constraint enforcement. Thus, β provides a tunable parameter to the SO to

model its tolerance on constraint violation. Similarly, the SO can encode her risk tolerance towards large uncertain costs by seeking to minimize $\mathrm{CVaR}_\alpha[f_{\boldsymbol{\omega}}(\boldsymbol{x})]$. This discussion motivates us to write the forward power procurement problem in Section 3.2 as a CVaR-penalized CVaR-constrained optimization program of the form

$$\begin{aligned} \mathscr{P}^0 : \underset{\boldsymbol{x}\in\mathbb{X}}{\text{minimize}} \quad & \mathrm{CVaR}_\alpha[f_{\boldsymbol{\omega}}(\boldsymbol{x})], \\ \text{subject to} \quad & \mathrm{CVaR}_{\beta^i}[g^i_{\boldsymbol{\omega}}(\boldsymbol{x})] \leq 0, \;\; i = 1,\ldots,p. \end{aligned} \tag{3.1}$$

Such problems have been studied in power systems for the optimal power flow (OPF) problem in [17].

In Section 3.3, we leverage our recent work in [18] to design an algorithm to solve the power procurement problem formulated as an instance of $\mathscr{P}^0$. The algorithm is an online primal-dual stochastic subgradient method. In each iteration, we obtain two new samples and update the primal and dual variables using these samples. Our result, adapted from [18, Theorem 2], provides a bound on the expected distance to optimality and constraint violation for $\mathscr{P}^0$ after a fixed number of iterations. The iteration and sample complexity grow with the risk parameters $\alpha, \boldsymbol{\beta} := (\beta^1,\ldots,\beta^p)$. The algorithm design is motivated by the fact that predictions of wind power output typically depend on Monte Carlo runs of complex weather models. While samples are easy to obtain, an explicit description of the underlying probability distribution on wind power output is challenging to characterize. Furthermore, computing the CVaR of f or g's for every possible dispatch decision with respect to that distribution can prove difficult. Our algorithm circumvents these difficulties by taking a primal-dual step based on the samples. Section 3.4 provides results from our numerical experiments on an illustrative two-bus network example. Section **??** concludes the chapter with directions for future work.

We remark that chance-constrained programs with constraints defined as

$$\mathbb{P}[g^i_{\boldsymbol{\omega}}(\boldsymbol{x}) \leq 0] \geq 1 - \boldsymbol{\varepsilon}^i$$

provides an alternate design paradigm for an SO to specify a tolerance on possible constraint violations. Since its introduction by Charnes and Cooper in [19], it has found extensive applications in engineering decision-making, including forward power procurement problems in power systems [20, 21] as well as OPF [22] and reserve scheduling problems [23]. Chance-constrained formulations are typically nonconvex even if the functions f and g's are convex, making it difficult to provide optimality guarantees, unlike our advocated CVaR-based counterparts.

This chapter is based on [24]. A detailed description of the algorithm and associated proofs can be found in [18].

3.2 Forward power procurement problem formulation

In this section, we formulate the risk-sensitive forward power procurement problem using conditional value at risk (CVaR). We begin by describing the deterministic variant that proves useful to present the risk-sensitive counterpart next.

3.2.1 A deterministic power procurement problem

Consider an electric power network on n buses, labeled $1,\ldots,n$, and m transmission lines. Let each bus be equipped with a dispatchable generator, a wind power producer and a load. Denote the vector of nodal dispatchable power productions by $\boldsymbol{G} \in \mathbb{R}^n$, the vector of wind power productions by $\boldsymbol{\omega} \in \mathbb{R}^n$ and the nodal power demands by $\boldsymbol{D} \in \mathbb{R}^n$, where $\mathbb{R}$ is the set of real numbers. We adopt the DC approximation of power flow equations that assumes voltage magnitudes to be at their nominal values, ignores transmission line losses and deems small voltage phase angle differences between neighboring buses. With DC approximations, the (directed) power flows over the m transmission lines become linear functions of the vector of nodal power injections $\boldsymbol{x}$, given by $\boldsymbol{H}\boldsymbol{x}$. Here, $\boldsymbol{H} \in \mathbb{R}^{2m\times n}$ denotes the injection shift-factor (ISF) matrix which depends on the network topology and transmission line admittances. Let the (directed) power flow limits be denoted by $\boldsymbol{f}^{\mathsf{L}} \in \mathbb{R}^{2m}$. Given a known wind power output $\boldsymbol{\omega}$ and assuming a linear dispatch cost structure, the deterministic power procurement problem with DC approximations is described by

$$\begin{aligned} \mathscr{P}_{\text{det}}: \underset{\boldsymbol{G}}{\text{minimize}} \quad & \boldsymbol{c}^{\mathsf{T}}\boldsymbol{G}, \\ \text{subject to} \quad & \mathbb{1}^{\mathsf{T}}(\boldsymbol{G}-\boldsymbol{D}+\boldsymbol{\omega}) = 0, \\ & \boldsymbol{H}(\boldsymbol{G}-\boldsymbol{D}+\boldsymbol{\omega}) \le \boldsymbol{f}^{\mathsf{L}}, \\ & \underline{\boldsymbol{G}} \le \boldsymbol{G} \le \overline{\boldsymbol{G}}, \end{aligned} \tag{3.2}$$

where $\mathbb{1}$ denotes a vector of all ones of appropriate dimensions. The first two constraints model the set of feasible power injections and the last constraint ensures that dispatchable generation respects its capacity limits, described by $\overline{\boldsymbol{G}}, \underline{\boldsymbol{G}}$.

In practice, $\boldsymbol{\omega}$ is not known prior to the time of power delivery. The next section proposes a forward procurement problem that accounts for the uncertainty in $\boldsymbol{\omega}$.

3.2.2 The risk-sensitive counterpart

For the risk-sensitive forward procurement problem, the SO must determine the dispatch for a given realization of wind power output. That is, the dispatchable power production becomes a function of $\boldsymbol{\omega}$, denoted by $\boldsymbol{G}(\boldsymbol{\omega})$. Optimizing over general functions of $\boldsymbol{\omega}$ is challenging. Therefore, we restrict our attention to affine functions of $\boldsymbol{\omega}$ of the form

$$\boldsymbol{G}(\boldsymbol{\omega}) := \boldsymbol{G}^0 + \boldsymbol{G}^{\omega}(\boldsymbol{\omega})$$

with $\boldsymbol{G}^0 \in \mathbb{R}^n$ and $\boldsymbol{G}^{\omega} \in \mathbb{R}^{n\times n}$. Such a dispatch policy amounts to fixing a nominal dispatch $\boldsymbol{G}^0$ and a regulation to alter the output from that nominal dispatch as a linear function of the wind power output. As will be clear, while restriction of $\boldsymbol{G}(\boldsymbol{\omega})$ to affine functions of $\boldsymbol{\omega}$ results in a suboptimal power procurement, we retain convexity of the resulting optimization program, making it amenable to design efficient algorithms and analyze them.

With the above affine dispatch structure, we now define our risk-sensitive forward power procure-

ment problem.

$$\begin{aligned}\mathscr{P}_{\text{risk}}: \underset{\boldsymbol{G}^0,\boldsymbol{G}^\omega}{\text{minimize}} \quad & \text{CVaR}_\alpha\left[\boldsymbol{c}^\intercal(\boldsymbol{G}^0+\boldsymbol{G}^\omega\boldsymbol{\omega})\right], \\ \text{subject to} \quad & \mathbb{1}^\intercal(\boldsymbol{G}^0+\boldsymbol{G}^\omega\boldsymbol{\omega}-\boldsymbol{D}+\boldsymbol{\omega})=0 \ \text{ a.s.}, \\ & \text{CVaR}_{\beta^{\mathsf{L}}}\left[\boldsymbol{H}(\boldsymbol{G}^0+\boldsymbol{G}^\omega\boldsymbol{\omega}-\boldsymbol{D}+\boldsymbol{\omega})-\boldsymbol{f}^{\mathsf{L}}\right]\leq 0, \\ & \text{CVaR}_{\beta^{\mathsf{G}}}\left[-\boldsymbol{G}^0-\boldsymbol{G}^\omega\boldsymbol{\omega}+\underline{\boldsymbol{G}}\right]\leq 0, \\ & \text{CVaR}_{\beta^{\mathsf{G}}}\left[\boldsymbol{G}^0+\boldsymbol{G}^\omega\boldsymbol{\omega}-\overline{\boldsymbol{G}}\right]\leq 0.\end{aligned} \tag{3.3}$$

In the above problem, CVaR on a vector argument is interpreted elementwise. We enforce power balance in a robust fashion, but allow flexibility in meeting line capacity and generation capacity constraints. Line capacity limits arise primarily from thermal considerations and can be relaxed for short durations; see [12] for discussion. Since we relax generation capacity limits in $\mathscr{P}_{\text{risk}}$, the SO may be unable to reliably meet demand requirements for certain realizations of wind. Thus, risk parameters β^{G} describe the SO's preference to maintain reliability in power delivery. We remark that there are alternate ways to enforce a risk-sensitive constraint on possible supply shortfall across scenarios, possibly including reserve capacities and load shedding. Consideration and comparison of such alternate formulations are relegated to future work.

3.3 Algorithm to solve $\mathscr{P}_{\text{risk}}$

In this section, we adopt our algorithm designed in our earlier work in [18] to solve $\mathscr{P}_{\text{risk}}$. The algorithm requires us to reformulate the almost sure enforcement of the power balance constraint to cast $\mathscr{P}_{\text{risk}}$ as an example of $\mathscr{P}^0$.

3.3.1 Reformulating $\mathscr{P}_{\text{risk}}$ as an instance of $\mathscr{P}^0$

Partition $\boldsymbol{G}^0$ and $\boldsymbol{G}^\omega$ as

$$\boldsymbol{G}^0 := \begin{pmatrix} G^0_s \\ \boldsymbol{G}^0_r \end{pmatrix}, \qquad \boldsymbol{G}^\omega := \begin{pmatrix} \boldsymbol{G}^\omega_s \\ \boldsymbol{G}^\omega_r \end{pmatrix}$$

where subscript s distinguishes the row corresponding to the slack bus in each, and r collects the rows for all other buses. Then, the power balance constraint yields

$$G^0_s + \boldsymbol{G}^\omega_s\boldsymbol{\omega} = -\mathbb{1}^\intercal\left(\boldsymbol{G}^0_r+\boldsymbol{G}^\omega_r\boldsymbol{\omega}\right)+\mathbb{1}^\intercal(\boldsymbol{D}-\boldsymbol{\omega}). \tag{3.4}$$

Conformally partition $\boldsymbol{c}, \boldsymbol{D}$ and $\boldsymbol{\omega}$. Also, partition $\boldsymbol{H} := \begin{pmatrix} \boldsymbol{H}_s & \boldsymbol{H}_r \end{pmatrix}$ along its columns, distinguishing the one corresponding to the slack bus from the rest. Then, we have

$$\begin{aligned}&\boldsymbol{H}(\boldsymbol{G}^0+\boldsymbol{G}^\omega\boldsymbol{\omega}-\boldsymbol{D}+\boldsymbol{\omega}) \\ &\quad= \begin{pmatrix} \boldsymbol{H}_s & \boldsymbol{H}_r \end{pmatrix}\begin{pmatrix} G^0_s+\boldsymbol{G}^\omega_s\boldsymbol{\omega}-D_s+\omega_s \\ \boldsymbol{G}^0_r+\boldsymbol{G}^\omega_r\boldsymbol{\omega}-\boldsymbol{D}_r+\boldsymbol{\omega}_r \end{pmatrix} \\ &\quad= \left(\boldsymbol{H}_r-\boldsymbol{H}_s\mathbb{1}^\intercal\right)\left(\boldsymbol{G}^0_r+\boldsymbol{G}^\omega_r\boldsymbol{\omega}-\boldsymbol{D}_r+\boldsymbol{\omega}_r\right).\end{aligned} \tag{3.5}$$

Finally, notice that

$$\boldsymbol{G}_r^{\omega}\boldsymbol{\omega} = \underbrace{\left(\boldsymbol{I}\otimes\boldsymbol{\omega}^{\intercal}\right)}_{:=\boldsymbol{W}}\underbrace{\mathsf{vec}\left([\boldsymbol{G}_r^{\omega}]^{\intercal}\right)}_{:=\boldsymbol{\Gamma}_r^{\omega}}, \tag{3.6}$$

where $\mathsf{vec}(\cdot)$ stands for vectorization and $\otimes$ stands for the Kronecker product. Using (3.4) – (3.6), we reformulate $\mathscr{P}_{\text{risk}}$ in terms of $\boldsymbol{G}_r^0$ and $\boldsymbol{\Gamma}_r^{\omega}$ as

$$\begin{aligned}
&\underline{\mathscr{P}_{\text{risk}}}':\\
&\underset{\boldsymbol{G}_r^0,\boldsymbol{\Gamma}_r^{\omega}}{\text{minimize}} \quad \text{CVaR}_{\alpha}\left[(\boldsymbol{c}_r - c_s\mathbb{1})^{\intercal}(\boldsymbol{G}_r^0 + \boldsymbol{W}\boldsymbol{\Gamma}_r^{\omega}) + c_s\mathbb{1}^{\intercal}(\boldsymbol{D}-\boldsymbol{\omega})\right],\\
&\text{subject to} \quad \text{CVaR}_{\beta^{\mathsf{L}}}\left[(\boldsymbol{H}_r - \boldsymbol{H}_s\mathbb{1}^{\intercal})\right.\\
&\qquad\qquad \left.\cdot\left(\boldsymbol{G}_r^0 + \boldsymbol{W}\boldsymbol{\Gamma}_r^{\omega} - \boldsymbol{D}_r + \boldsymbol{\omega}_r\right) - \boldsymbol{f}^{\mathsf{L}}\right] \le 0,\\
&\qquad\qquad \text{CVaR}_{\beta^{\mathsf{G}}}\left[\mathbb{1}^{\intercal}(\boldsymbol{G}_r^0 + \boldsymbol{W}\boldsymbol{\Gamma}_r^{\omega} - \boldsymbol{D} + \boldsymbol{\omega}) + \underline{G}_s\right] \le 0,\\
&\qquad\qquad \text{CVaR}_{\beta^{\mathsf{G}}}\left[-\mathbb{1}^{\intercal}(\boldsymbol{G}_r^0 + \boldsymbol{W}\boldsymbol{\Gamma}_r^{\omega} - \boldsymbol{D} + \boldsymbol{\omega}) - \overline{G}_s\right] \le 0,\\
&\qquad\qquad \text{CVaR}_{\beta^{\mathsf{G}}}\left[-\boldsymbol{G}_r^0 - \boldsymbol{W}\boldsymbol{\Gamma}_r^{\omega} + \underline{\boldsymbol{G}}_r\right] \le 0,\\
&\qquad\qquad \text{CVaR}_{\beta^{\mathsf{G}}}\left[\boldsymbol{G}_r^0 + \boldsymbol{W}\boldsymbol{\Gamma}_r^{\omega} - \overline{\boldsymbol{G}}_r\right] \le 0.
\end{aligned} \tag{3.7}$$

The reformulation of $\mathscr{P}_{\text{risk}}$ in $\mathscr{P}_{\text{risk}}'$ reduces it to an instance of $\mathscr{P}^0$ over

$$\boldsymbol{x} := \begin{pmatrix}\boldsymbol{G}_r^0\\ \boldsymbol{\Gamma}_r^0\end{pmatrix}$$

with appropriate definitions of f and g's. We choose $\mathbb{X}$ in $\mathscr{P}^0$ as a box that contains reasonable values of $\boldsymbol{x}$. For example, $\boldsymbol{G}_r^0 \in [\underline{\boldsymbol{G}}_r, \overline{\boldsymbol{G}}_r]$ and $|\boldsymbol{\Gamma}_r^{\omega}| \le \mathsf{vec}\left(\overline{\boldsymbol{G}}_r^{\intercal}\otimes \text{diag}(\overline{\boldsymbol{\omega}})^{-1}\mathbb{1}\right)$, where $\overline{\boldsymbol{\omega}}$ denotes the vector of installed capacities for wind. Each element is bound by the wind capacity-normalized dispatchable generation capacity.

3.3.2 Algorithm to solve $\mathscr{P}^0$

Our exposition here mimics that in [18]. To provide insights into our algorithm design, we utilize the following variational characterization of CVaR.

$$\text{CVaR}_{\alpha}[f_{\boldsymbol{\omega}}(\boldsymbol{x})] = \underset{u\in\mathbb{R}}{\text{minimize}}\ \ \mathbb{E}[\psi_{\boldsymbol{\omega}}^f(\boldsymbol{x},u;\alpha)],$$

where

$$\psi_{\boldsymbol{\omega}}^f(\boldsymbol{x},u^f;\alpha) := \left\{u^f + \frac{1}{1-\alpha}[f_{\boldsymbol{\omega}}(\boldsymbol{x}) - u^f]^+\right\}, \tag{3.12}$$

and $[\cdot]^+$ computes the positive part of its argument. Utilizing a similar characterization for $\text{CVaR}_{\beta}^i[g_{\boldsymbol{\omega}}^i(\boldsymbol{x})]$ for $i = 1,\dots p$, we reformulate $\mathscr{P}^0$ as

$$\begin{aligned}
&\text{minimize} \quad \mathbb{E}[\psi_{\boldsymbol{\omega}}^f(\boldsymbol{x},u^f;\alpha)],\\
&\text{subject to} \quad \mathbb{E}[\psi_{\boldsymbol{\omega}}^{g^i}(\boldsymbol{x},u^{g^i};\beta^i)] \le 0,\ i = 1,\dots,p
\end{aligned} \tag{3.13}$$

Algorithm 2 Primal-dual stochastic subgradient method for $\mathscr{P}^0$.

1: **Initialize:**
Choose $\boldsymbol{x}_1 \in \mathbb{X}$, $\boldsymbol{z}_1 = 0$, and a positive sequence $\{\gamma_k\}$ and number of iterations K.

2: **for** $k = 1, \ldots, K$ **do**

3: Sample $\boldsymbol{\omega}_k \in \Omega$. Update $\boldsymbol{x}$, u^f, and $\boldsymbol{u}^{\boldsymbol{g}}$ as

$$\boldsymbol{x}_{k+1} \leftarrow \underset{\boldsymbol{x}\in\mathbb{X}}{\operatorname{argmin}} \left\langle \frac{\nabla f_{\boldsymbol{\omega}_k}(\boldsymbol{x}_k)}{1-\alpha} \mathbb{I}_{\{f_{\boldsymbol{\omega}_k}(\boldsymbol{x}_k)\geq u_k^f\}} + \sum_{i=1}^{m} \frac{z_k^i \nabla g^i_{\boldsymbol{\omega}_k}(\boldsymbol{x}_k)}{1-\beta_i} \mathbb{I}_{\{g^i_{\boldsymbol{\omega}_k}(\boldsymbol{x}_k)\geq u_k^f\}}, \boldsymbol{x} - \boldsymbol{x}_k \right\rangle + \frac{1}{2\gamma_k} \|\boldsymbol{x} - \boldsymbol{x}_k\|^2, \tag{3.8}$$

$$u_{k+1}^f \leftarrow \underset{u^f\in\mathbb{U}^f}{\operatorname{argmin}} \left\langle 1 - \frac{1}{1-\alpha} \mathbb{I}_{\{f_{\boldsymbol{\omega}_k}(\boldsymbol{x}_k)\geq u_k^f\}}, u^f - u_k^f \right\rangle + \frac{1}{2\gamma_k} \left\| u^f - u_k^f \right\|^2, \tag{3.9}$$

$$\boldsymbol{u}_{k+1}^{\boldsymbol{g}} \leftarrow \underset{\boldsymbol{u}^{\boldsymbol{g}}\in\mathbb{U}^{\boldsymbol{g}}}{\operatorname{argmin}} \left\langle \mathbb{1} - \operatorname{diag}(\mathbb{1}-\boldsymbol{\beta})^{-1} \mathbb{I}_{\{\boldsymbol{g}_{\boldsymbol{\omega}_k}(\boldsymbol{x}_k)\geq \boldsymbol{u}_k^{\boldsymbol{g}}\}}, \boldsymbol{u}^{\boldsymbol{g}} - \boldsymbol{u}_k^{\boldsymbol{g}} \right\rangle + \frac{1}{2\gamma_k} \left\| \boldsymbol{u}^{\boldsymbol{g}} - \boldsymbol{u}_k^{\boldsymbol{g}} \right\|^2. \tag{3.10}$$

4: Sample $\boldsymbol{\omega}_{k+1/2} \in \Omega$. Update $\boldsymbol{z}$ as

$$\boldsymbol{z}_{k+1} \leftarrow \underset{\boldsymbol{z}\in\mathbb{R}^m_+}{\operatorname{argmax}} \left\langle \boldsymbol{u}^{\boldsymbol{g}} + \operatorname{diag}(\mathbb{1}-\boldsymbol{\beta})^{-1} [\boldsymbol{g}_{\boldsymbol{\omega}_{k+1/2}}(\boldsymbol{x}_{k+1}) - \boldsymbol{u}^{\boldsymbol{g}}]^+, \boldsymbol{z} - \boldsymbol{z}_k \right\rangle - \frac{1}{2\gamma_k} \|\boldsymbol{z} - \boldsymbol{z}_k\|^2. \tag{3.11}$$

5: **end for**

over $\boldsymbol{x} \in \mathbb{X}$, $u^f \in \mathbb{U}^f$ and $\boldsymbol{u}^{\boldsymbol{g}} \in \mathbb{U}^{\boldsymbol{g}}$. We compute $\mathbb{U}^f$ and $\mathbb{U}^{\boldsymbol{g}}$ from the observation that a solution of $\mathscr{P}^0$ can only admit solutions with u^f and $\boldsymbol{u}^{\boldsymbol{g}}$ that take values between the minimum and maximum of the functions f and g as $\boldsymbol{x}, \boldsymbol{\omega}$ vary over the compact sets $\mathbb{X}$ and Ω. Algorithm 2 formally presents our method to solve (3.13) that implements a projected stochastic primal-dual subgradient update with two samples per iteration. Here, $\boldsymbol{z} \in \mathbb{R}^p_+$ denotes the vector of Lagrange multipliers associated with the inequality constraints in (3.13), $\mathbb{I}$ is the indicator function, and $\langle \cdot, \cdot \rangle$ stands for the usual inner product. Our sampling-based algorithm does not require the knowledge of the distribution on $\boldsymbol{\omega}$. Unlike other sampling-based techniques proposed for chance-constrained problems in [25, 26], which require the samples to be computed prior to solving the optimization problem, our algorithm is online and optimizes with streaming samples.

3.3.3 Convergence guarantees of Algorithm 2 for $\mathscr{P}^0$

To present the result, we compute bounds C_f, C_G^i and D_G^i in Figure 3.1 on the 2-norms of subgradients $\nabla f_{\boldsymbol{\omega}}$, $\nabla g^i_{\boldsymbol{\omega}}$ and the function value $g^i_{\boldsymbol{\omega}}$, respectively, for our problem. Here, $|\cdot|$ denotes the element-wise absolute value. Derivations are omitted due to space constraints. Letting $\boldsymbol{x}^*, \boldsymbol{z}^*$ denote the primal-dual optimizer of $\mathscr{P}^0$, we further utilize these constants to define $P_1, P_2(\alpha, \boldsymbol{\beta})$ and $P_3(\alpha, \boldsymbol{\beta})$ in Figure 3.1 that proves useful in stating the result.

$$C_f := \|\boldsymbol{c}_r - c_s\mathbb{1}\|\|\overline{\boldsymbol{\omega}}\|,\ \boldsymbol{C}_g := \begin{pmatrix} \|\boldsymbol{H}_r - \boldsymbol{H}_s\mathbb{1}^\intercal\| \\ \sqrt{n-1} \\ \sqrt{n-1} \\ \mathbb{1} \\ \mathbb{1} \end{pmatrix} \left(\sqrt{n-1} + \|\overline{\boldsymbol{\omega}}\|\right),$$

$$\boldsymbol{D}_g := \begin{pmatrix} \boldsymbol{f}^\perp + |\boldsymbol{H}_r - \boldsymbol{H}_s\mathbb{1}^\intercal|(\overline{\boldsymbol{G}}_r + \mathbb{1}\overline{\boldsymbol{\omega}}^\intercal\mathbb{1} - \boldsymbol{D} + \overline{\boldsymbol{\omega}}) \\ \mathbb{1}^\intercal(\overline{\boldsymbol{G}}_r + \mathbb{1}\overline{\boldsymbol{\omega}}^\intercal\mathbb{1} - \boldsymbol{D} + \overline{\boldsymbol{\omega}}) - \underline{\boldsymbol{G}}_s \\ \mathbb{1}^\intercal(\overline{\boldsymbol{G}}_r + \mathbb{1}\overline{\boldsymbol{\omega}}^\intercal\mathbb{1} - \boldsymbol{D} + \overline{\boldsymbol{\omega}}) + \overline{\boldsymbol{G}}_s \\ \overline{\boldsymbol{G}}_r - \underline{\boldsymbol{G}}_r + \mathbb{1}\overline{\boldsymbol{\omega}}^\intercal\mathbb{1} \\ \overline{\boldsymbol{G}}_r - \underline{\boldsymbol{G}}_r + \mathbb{1}\overline{\boldsymbol{\omega}}^\intercal\mathbb{1} \end{pmatrix},$$

$$P_1 := 2\|\boldsymbol{x}_1 - \boldsymbol{x}_*\|^2 + 4\|\mathbb{1} + \boldsymbol{z}_*\|^2,\ P_2(\alpha,\beta) := \frac{16(C_f^2+1)}{(1-\alpha)^2} + 2\left\|\operatorname{diag}(\mathbb{1}+\beta)\operatorname{diag}(\mathbb{1}-\beta)^{-1}\boldsymbol{D}_g\right\|^2,$$

$$P_3(\alpha,\beta) := 16p\left\|\operatorname{diag}(\mathbb{1}-\beta)^{-1}\boldsymbol{C}_g\right\|^2 + 16p\left\|\operatorname{diag}(\mathbb{1}-\beta)^{-1}\mathbb{1}\right\|^2.$$

Figure 3.1: Constants associated with $\mathscr{P}_{\text{risk}}$.

Proposition 3 (Convergence result for $\mathscr{P}^0$)**.** *Given $\varepsilon > 0$ and let p_*^0 denote the optimal value of $\mathscr{P}^0$, and K_* and $\gamma_k = \gamma_*/\sqrt{K_*}$ for $k = 1,\ldots,K_*$, where K_* and γ_* satisfy the following with $y = 1 + \frac{P_2}{P_1P_3}$,*

$$\gamma_*^2 = \frac{2P_3^{-1}}{2+y+\sqrt{y^2+8y}},\ K_* = \frac{(P_1+P_2\gamma_*^2)^2}{16\gamma_*^2(1-P_3\gamma_*^2)^2\varepsilon^2}. \tag{3.14}$$

Then, the iterates generated by Algorithm 2 on $\mathscr{P}^0$ with parameters α and β satisfy

$$\mathbb{E}[CVaR_\alpha(f_\omega(\overline{\boldsymbol{x}}_{K_*+1}))] - p_*^0 \le \varepsilon, \tag{3.15}$$

$$\mathbb{E}[CVaR_{\beta^i}(g_\omega^i(\overline{\boldsymbol{x}}_{K_*+1}))] \le \varepsilon \tag{3.16}$$

where, $\overline{\boldsymbol{x}}_{K_*} = \frac{1}{K_*}\sum_{k=1}^{K_*}\boldsymbol{x}_k$.

Thus, our result provides guarantees on suboptimality and constraint violation in expectation, where the expectation is computed with respect to the stochastic dynamics of the algorithm. Additionally, while P_1 is typically not known a priori, Theorem 3 still guarantees convergence of Algorithm 2 with an upper bound on P_1. The iteration count K_* increases with the risk-aversion parameters α, β.

The proposed algorithm is a stochastic subgradient method. These methods are rate-limited to $\mathscr{O}(1/\sqrt{K})$ and are typically slow to converge. Unfortunately, non-smoothness of ψ in (3.12) limits us to use slow subgradient methods.

3.4 An illustrative two-bus network example

We apply Algorithm 2 to $\mathscr{P}_{\text{risk}}$ on a two-bus network in Figure 3.2. Wind output from two wind power plants from the New York area were taken from NREL's synthetic dataset [27], treating the

pair of wind power outputs every 5 minutes over 2008-2011 as a single sample ω. In practice, these samples would be output from weather models which would account for diurnal/seasonal variation. Simulations were performed on an AWS m5.xlarge instance.

The buses are equipped with 40 and 20 MW of wind capacity, respectively. The results of Algorithm 2 with $\varepsilon = 0.1$ for various choices of $\alpha, \beta's$ are shown in Table 3.1.

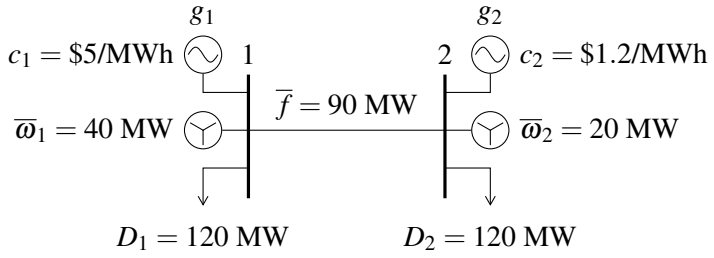

Figure 3.2: The two-bus network example.

Increasing risk-aversion towards constraints results in a reduction in the associated violation, while also incurring greater cost of generation. Similarly, increasing aversion towards cost results in decreased worst-case cost. Thus, these values capture the trade-off between cost and reliability of constraint satisfaction.

Aversion	α	β^{L}	β^{G}	Highest Dispatch Cost ($)	Worst-Case Const. Violation Line (MW)	Worst-Case Const. Violation Generation (MW)	Iterations ($\times 10^9$)	Runtime (s)
None	0	0	0	400	25	24	2.9	3767
Line capacity	0	0.6	0.2	402	0	50	9.2	21400
Dispatch cost	0.6	0.2	0.2	352	13	0	4.6	9660

Table 3.1: Results of Algorithm 2 for the two-bus network example.

4. Pricing Conditional Value at Risk-Sensitive Power Procurement

4.1 Introduction

Deepening penetration of uncertain renewable generation in electric power networks introduces greater supply-side uncertainty. Historically, uncertainty in demand/supply in economic dispatch (ED) formulations has been accommodated in a rather ad hoc manner, e.g., by planning for the nominal scenario and choosing fixed reserve margins to deal with forecast errors. Unfortunately, increasing renewable penetration ultimately leads to greater forecast errors and prohibitively large reserve margins. Instead, recent work makes use of considerable effort focused on obtaining probabilistic forecasts of variable renewable generation that capture spatio-temporal variations [28]. These efforts explicitly model uncertainty, optimize against it, and define pricing mechanisms to support that optimization, e.g., in [29–35]. In this chapter, we study the question of defining prices for electricity in a risk-sensitive ED problem. We model risk via the popular conditional value-at-risk (CVaR) measure [14, 36]. Our key contribution is the definition and analysis of locational marginal prices from a CVaR-sensitive ED problem. This chapter is based on the work in [37] that contains the proofs of the various claims.

Why CVaR? While this risk measure has seen widespread adoption in finance and gained traction in engineering applications, it has received limited attention in power systems. Examples include [9,24,38]. CVaR benefits from being a coherent risk measure, which ensures that the risk-sensitive problem retains the convexity of the deterministic variant, irrespective of the distribution of the underlying uncertainty. Convexity is a useful property for two reasons: it permits the design of efficient algorithms via sampling, and the mature duality theory of convex programming allows the derivation and analysis of meaningful prices for electricity.

In this chapter, we begin by presenting the CVaR-based ED problem which imposes risk-sensitive network and generation limits in Section 4.2. We adopt the perspective of a system operator (SO) solving the ED problem to manage operational and power delivery risks across the network. CVaR is equipped with a tunable parameter, enabling the SO to tradeoff economic efficiency and network security with varying levels of conservativeness. In Section 4.3, we apply duality theory to define risk-sensitive locational marginal prices (risk-LMPs). These prices endogenize stochasticity of renewable generation and compensate dispatchable generators for nominal generation and regulation commitments in response to forecast errors. Our prices reduce to conventional LMPs as the forecast error goes to zero. Section 4.4 presents a sample average approximation (SAA) approach to solving the CVaR-sensitive dispatch and prices. We demonstrate key properties of the prices through a numerical example on a five-bus power network. Finally, Section 4.5 addresses revenue adequacy of our settlement process.

4.2 The CVaR-sensitive ED problem

We consider a power network with n buses connected by ℓ lines. Each bus is equipped with some dispatchable generation, non-dispatchable (renewable) infeeds, and inflexible demand, the nodal values of which are collected in the vectors, $\boldsymbol{g}$, $\boldsymbol{\xi}$, and $\boldsymbol{d}$, respectively. Dispatchable generators are those whose output can be altered on command, such as conventional thermal and hydro-electric plants. The nodal renewable power injection, $\boldsymbol{\xi}$, is random and takes values over a compact set, $\boldsymbol{\Xi}$. These samples, $\boldsymbol{\xi}$, can be obtained, either from historical measurements (e.g., the NREL wind database) or from generative models (e.g., generative adversarial networks in [39]).

Accommodating uncertainty in renewable availablility, we formulate an ED problem that schedules both nominal dispatch and a power output adjustment (reserve policies) for dispatchable generators, allowing generators to respond to forecast errors in renewable supply by making $\boldsymbol{g}$ depend on $\boldsymbol{\xi}$. We restrict attention to affine recourse policies, i.e.,

$$\boldsymbol{g}(\boldsymbol{\xi}) = \boldsymbol{g}_0 - \boldsymbol{G}\Delta\boldsymbol{\xi}, \tag{4.1}$$

where $\boldsymbol{g}_0$ is the nominal generation, $\boldsymbol{\xi}_0$ the nominal or forecasted renewable infeeds and $\boldsymbol{G}$ encodes the adjustments to forecast errors $\Delta\boldsymbol{\xi} := (\boldsymbol{\xi} - \boldsymbol{\xi}_0)$. Specifically, with n wind resources in the system, $\boldsymbol{G} \in \mathbb{R}^{n\times n}$ and G_{ij} denotes the portion of deviation in renewable generation $\Delta\xi_j$ at node j picked up by generator at node i. Here, $\mathbb{R}$ is the set of real numbers. Note that our recourse policy here is slightly different from that in Chapter 3. We retain this version to keep it consistent with our published work in [37]. Assume that forecast errors are zero-mean, i.e.,

$$\mathbb{E}[\Delta\boldsymbol{\xi}] = 0. \tag{4.2}$$

We enforce three types of constraints: network-wide power balance, generation capacity limits, and transmission line flow limits. We adopt a linear power flow model via the widely used DC approximations that assume small voltage angle differences between nodes, lossless lines and (per unit) voltage magnitudes close to unity. Under these assumptions, reactive power is neglected and line flows become linear maps of the power injections across the network.

Power balance across the network for all $\boldsymbol{\xi}$ requires $\mathbb{1}^\mathsf{T}(\boldsymbol{g}(\boldsymbol{\xi}) + \boldsymbol{\xi} - \boldsymbol{d}) = 0$, where $\mathbb{1}$ is the vector of all ones of appropriate size. Under an affine recourse policy and assuming zero-mean forecast errors, this is equivalent to

$$\mathbb{1}^\mathsf{T}(\boldsymbol{g}_0 + \boldsymbol{\xi}_0 - \boldsymbol{d}) = 0, \quad \boldsymbol{G}^\mathsf{T}\mathbb{1} = \mathbb{1}. \tag{4.3}$$

Dispatchable generators can only produce power within their capacities, i.e., within $[0, \overline{\boldsymbol{g}}]$. Instead of requiring these capacity limits be met for each $\boldsymbol{\xi}$, we enforce them in a risk-sensitive fashion using CVaR. To describe the modeling approach, consider a scalar random variable, Z, with a continuous cumulative distribution, F. Then, $\mathrm{CVaR}_\delta[Z]$ is the expectation over the $(1-\delta)$-tail of the distribution,

$$\mathrm{CVaR}_\delta[Z] := \mathbb{E}[Z \mid Z \geq F^{-1}(\delta)].$$

Here, $\mathbb{E}$ stands for the expectation operator and δ is a tunable parameter that takes values in $[0,1)$. As $\delta \downarrow 0$, $\text{CVaR}_\delta[Z]$ becomes the average value of Z. Taking $\delta \uparrow 1$, it approaches the highest value that Z can take. CVaR over arbitrary distributions is defined via the following variational characterization by Rockafellar and Uryasev in [14].

$$\text{CVaR}_\delta[Z] := \underset{u\in\mathbb{R}}{\text{minimum}} \left\{ u + \frac{1}{1-\delta}\mathbb{E}[(Z-u)^+] \right\}, \tag{4.4}$$

where $[A]^+$ is the positive part of A. Equipped with this definition, we impose risk-sensitive local generation constraints,

$$\text{CVaR}_\gamma[\boldsymbol{g}_0 - \boldsymbol{G}\Delta\boldsymbol{\xi}] \le \overline{\boldsymbol{g}}, \quad \text{CVaR}_\gamma[-\boldsymbol{g}_0 + \boldsymbol{G}\Delta\boldsymbol{\xi}] \le \boldsymbol{0} \tag{4.5}$$

for a parameter $\gamma \in [0,1)$. The CVaR-based constraints in the above relation are imposed element-wise. As $\gamma \uparrow 1$, constraints become tighter, requiring generation limits to be imposed for almost every sample. However, when $\gamma \downarrow 0$, constraints are only enforced on average, allowing for the potential inability to respond to uncertain wind across multiple scenarios.

To enforce risk-sensitive line flow constraints, let $\boldsymbol{H} \in \mathbb{R}^{2\ell\times n}$ denote the (directed) injection shift factor matrix. Under the linear power flow model, the directed flows across the network are $\boldsymbol{H}(\boldsymbol{g}(\boldsymbol{\xi}) + \boldsymbol{\xi} - \boldsymbol{d})$. Denoting the (directed) line flow capacity limits by $\boldsymbol{f} \in \mathbb{R}^{2\ell}$, we impose

$$\text{CVaR}_\beta\left[\boldsymbol{H}\left(\boldsymbol{g}_0 - \boldsymbol{G}\Delta\boldsymbol{\xi} + \boldsymbol{\xi} - \boldsymbol{d}\right)\right] \le \boldsymbol{f} \tag{4.6}$$

for risk parameter $\beta \in [0,1)$. Altogether, the CVaR-sensitive ED problem can be formulated as

$$\underset{\boldsymbol{g}_0,\boldsymbol{G}}{\text{minimum}} \;\; \boldsymbol{c}^\mathsf{T}\boldsymbol{g}_0, \;\; \text{subject to} \;\; (4.3), (4.5), (4.6). \tag{4.7}$$

Here, we seek to minimize a linear procurement cost, where $\boldsymbol{c}$ is the vector of offer prices submitted by all generators. We assume that renewable power suppliers are price-takers, offering energy at zero marginal cost. It can be seen that

$$\boldsymbol{c}^\mathsf{T}\boldsymbol{g}_0 = \mathbb{E}[\boldsymbol{c}^\mathsf{T}(\boldsymbol{g}_0 - \boldsymbol{G}\Delta\boldsymbol{\xi})] = \mathbb{E}[\boldsymbol{c}^\mathsf{T}\boldsymbol{g}(\boldsymbol{\xi})],$$

owing to the zero-mean forecast error assumption in (4.2). Thus, (4.7) seeks to minimize expected generation costs, while imposing risk-sensitive constraints. By virtue of coherence, the CVaR-sensitive ED problem in (4.7) is a convex optimization problem, regardless of the distribution of $\boldsymbol{\xi}$.

Remark 1. *CVaR-sensitive constraints are intimately related to chance-constraints. Specifically, CVaR-sensitive constraints are inner approximations of chance constraints, i.e.,*

$$\mathit{CVaR}_\beta[Z] \le 0 \Rightarrow \mathbb{P}\{Z \le 0\} \ge \beta$$

for a scalar random variable Z. Chance-constrained formulations typically require assumptions on the distribution to admit convex reformulations, while those that are CVaR-sensitive do not. By nature, chance constraints seek to control the frequency of constraint violations, while CVaR-sensitive constraints control both the frequency and severity of violations.

4.3 Risk-sensitive locational marginal prices (risk-LMPs) and the settlement process

We now proceed to define prices for electricity from the CVaR-sensitive ED problem in (4.7). To that end, we first reformulate (4.7) using the characterization of CVaR in (4.4).

$$
\begin{aligned}
J^\star(\boldsymbol{d}) \;:=\; & \underset{\boldsymbol{g}_0,\boldsymbol{G},\boldsymbol{u},\underline{\boldsymbol{v}},\overline{\boldsymbol{v}}}{\text{minimum}} \;\; \boldsymbol{c}^\intercal \boldsymbol{g}_0, && \text{(4.8a)}\\
& \text{subject to} \\
& \mathbb{1}^\intercal(\boldsymbol{g}_0 + \boldsymbol{\xi}_0 - \boldsymbol{d}) = 0, && \text{(4.8b)}\\
& \boldsymbol{G}^\intercal \mathbb{1} = \mathbb{1}, && \text{(4.8c)}\\
& \boldsymbol{u} + \frac{1}{1-\beta}\mathbb{E}\left[(\boldsymbol{H}(\boldsymbol{g}_0 - \boldsymbol{G}\Delta\boldsymbol{\xi} + \boldsymbol{\xi} - \boldsymbol{d}) - \boldsymbol{u})^+\right] \\
& \qquad \leq \boldsymbol{f}, && \text{(4.8d)}\\
& \underline{\boldsymbol{v}} + \frac{1}{1-\gamma}\mathbb{E}\left[(-\boldsymbol{g}_0 + \boldsymbol{G}\Delta\boldsymbol{\xi} - \underline{\boldsymbol{v}})^+\right] \leq 0, && \text{(4.8e)}\\
& \overline{\boldsymbol{v}} + \frac{1}{1-\gamma}\mathbb{E}\left[(\boldsymbol{g}_0 - \boldsymbol{G}\Delta\boldsymbol{\xi} - \overline{\boldsymbol{g}} - \overline{\boldsymbol{v}})^+\right] \leq 0. && \text{(4.8f)}
\end{aligned}
$$

Associate Lagrange multipliers $\lambda, \boldsymbol{\nu}$ and $\boldsymbol{\mu}$ with constraints (4.8b),(4.8c) and (4.8d), respectively. Let $z^\star$ denote the optimal value of any (primal or dual) variable z in (4.8).

Definition 1. *The vector of risk-sensitive locational marginal prices (risk-LMPs) is defined as*

$$\boldsymbol{\pi} := \lambda^\star \mathbb{1} - \boldsymbol{H}^\intercal \boldsymbol{\mu}^\star. \tag{4.9}$$

These prices are nodally uniform, i.e., the prices can vary across buses, but the same price π_i is observed by all participants at bus i. Our definition of risk-LMPs mimics that of LMPs derived from a deterministic ED problem (e.g., see [40]). Risk-LMPs comprise of two terms–$\lambda^\star\mathbb{1}$ and $\boldsymbol{H}^\intercal\boldsymbol{\mu}^\star$. The first defines a common base price across the network that emanates from the network-wide power balance constraint for the nominal scenario. The second term arises due to congestion and introduces locational dependency. Unlike the deterministic case, the congestion component in the CVaR-sensitive problem does not only depend on the nominal dispatch. That is, adverse scenarios can result in a non-zero congestion component despite an uncongested nominal dispatch.

Our first result relates risk-LMPs to the sensitivity of the optimal cost of (4.8) to nodal demands–a result that holds for LMPs derived from a deterministic ED problem.

Proposition 4. *$J^\star$ is convex in $\boldsymbol{d}$. Suppose $\boldsymbol{X}^\star := (\boldsymbol{H} - \boldsymbol{H}\boldsymbol{G}^\star)\Delta\boldsymbol{\xi}$ has a smooth cumulative distribution function and the optimal set of Lagrange multipliers of* (4.8) *is bounded. Then, $\boldsymbol{\pi} \in \partial_{\boldsymbol{d}} J^\star(\boldsymbol{d})$, where $\partial_{\boldsymbol{d}}$ computes the subdifferential set of $J^\star$.*

The pricing mechanism is incomplete without defining a settlement process, i.e., how every market participant is compensated under risk-LMPs. We adopt a similar model to existing literature for

consumers, wherein they are charged $\pi_i d_i$ for consuming quantity d_i at bus i. Under the risk-sensitive model, generators incur an additional cost of maintaining reserve capacity in the form of $\boldsymbol{G}\Delta\boldsymbol{\xi}$ and must be compensated accordingly. We propose the dual multiplier $\boldsymbol{\nu}^\star$ to reflect the price of maintaining this reserve capacity. Thus, each generator i is paid $\pi_i[g_0^\star]_i$ for the nominal cost of generation and $\sum_{j=1}^n G_{ij}^\star \nu_i^\star$ for maintaining reserve capacity. On the other hand, renewable supplier i is paid $\pi_i[\xi_0]_i - \nu_i^\star$, corresponding to a payment for nominal supply and a penalty levied for their induced uncertainty. The penalty reflects the principle of *cost allocation based on cost causation*.

4.4 Solving the CVaR-sensitive ED problem using sample average approximation

We compute the dispatch and prices from (4.8) using N independent and identically distributed (iid) samples of renewable generation $\boldsymbol{\xi}^1, \ldots, \boldsymbol{\xi}^N$ as follows. We replace the expectations with empirical means in each constraint, e.g., the empirical mean variant of (4.8d) can be reformulated as

$$\begin{aligned}
&\boldsymbol{u} + \frac{1}{N(1-\beta)} \sum_{j=1}^{N} \left[\left(\boldsymbol{H}(\boldsymbol{g}_0 - \boldsymbol{G}\Delta\boldsymbol{\xi}^j + \boldsymbol{\xi}^j - \boldsymbol{d}) - \boldsymbol{u} \right)^+ \right] \leq \boldsymbol{f} \\
&\equiv \begin{cases} \boldsymbol{u} + \frac{1}{N(1-\beta)} \sum_{j=1}^{N} \boldsymbol{t}^j \leq \boldsymbol{0}, \\ \boldsymbol{t}^j \geq \boldsymbol{H}(\boldsymbol{g}_0 - \boldsymbol{G}\Delta\boldsymbol{\xi}^j + \boldsymbol{\xi}^j - \boldsymbol{d}) - \boldsymbol{f} - \boldsymbol{u}, \quad \boldsymbol{t}^j \geq 0. \end{cases}
\end{aligned}$$

Proceeding similarly with (4.8e)–(4.8f), we arrive at the following SAA-based CVaR-sensitive ED problem.

$$\begin{aligned}
\widehat{J}_N^\star(\boldsymbol{d}) := \text{minimize} \quad & \boldsymbol{c}^\mathsf{T}\boldsymbol{g}_0, && \text{(4.10a)} \\
\text{subject to} \quad & \\
& \mathbb{1}^\mathsf{T}(\boldsymbol{g}_0 + \boldsymbol{\xi}_0 - \boldsymbol{d}) = 0, && \text{(4.10b)} \\
& \boldsymbol{G}^\mathsf{T}\mathbb{1} = \mathbb{1}, && \text{(4.10c)} \\
& \boldsymbol{u} + \frac{1}{(1-\beta)N} \sum_{j=1}^{N} \boldsymbol{t}^j \leq \boldsymbol{0}, && \text{(4.10d)} \\
& \boldsymbol{t}^j \geq \boldsymbol{H}(\boldsymbol{g}_0 - \boldsymbol{G}\Delta\boldsymbol{\xi}^j + \boldsymbol{\xi}^j - \boldsymbol{d}) - \boldsymbol{f} - \boldsymbol{u}, && \text{(4.10e)} \\
& \underline{\boldsymbol{v}} + \frac{1}{(1-\gamma)N} \sum_{j=1}^{N} \underline{\boldsymbol{s}}^j \leq \boldsymbol{0}, && \text{(4.10f)} \\
& \underline{\boldsymbol{s}}^j \geq -\boldsymbol{g}_0 + \boldsymbol{G}\Delta\boldsymbol{\xi}^j - \underline{\boldsymbol{v}}, && \text{(4.10g)} \\
& \overline{\boldsymbol{v}} + \frac{1}{(1-\gamma)N} \sum_{j=1}^{N} \overline{\boldsymbol{s}}^j \leq \boldsymbol{0}, && \text{(4.10h)} \\
& \overline{\boldsymbol{s}}^j \geq \boldsymbol{g}_0 - \boldsymbol{G}\Delta\boldsymbol{\xi}^j - \overline{\boldsymbol{g}} - \overline{\boldsymbol{v}}, && \text{(4.10i)} \\
& \boldsymbol{t}^j, \underline{\boldsymbol{s}}^j, \overline{\boldsymbol{s}}^j \geq \boldsymbol{0}, \quad j = 1, \ldots, N
\end{aligned}$$

over $\boldsymbol{g_0}, \boldsymbol{G}, \boldsymbol{u}, \boldsymbol{t}^j, \underline{\boldsymbol{v}}, \overline{\boldsymbol{v}}, \underline{\boldsymbol{s}}^j, \overline{\boldsymbol{s}}^j$. In effect, (4.10) is an approximation to (4.8) for computing an optimal dispatch. This SAA-based ED problem can be solved as a linear program. Linear programming

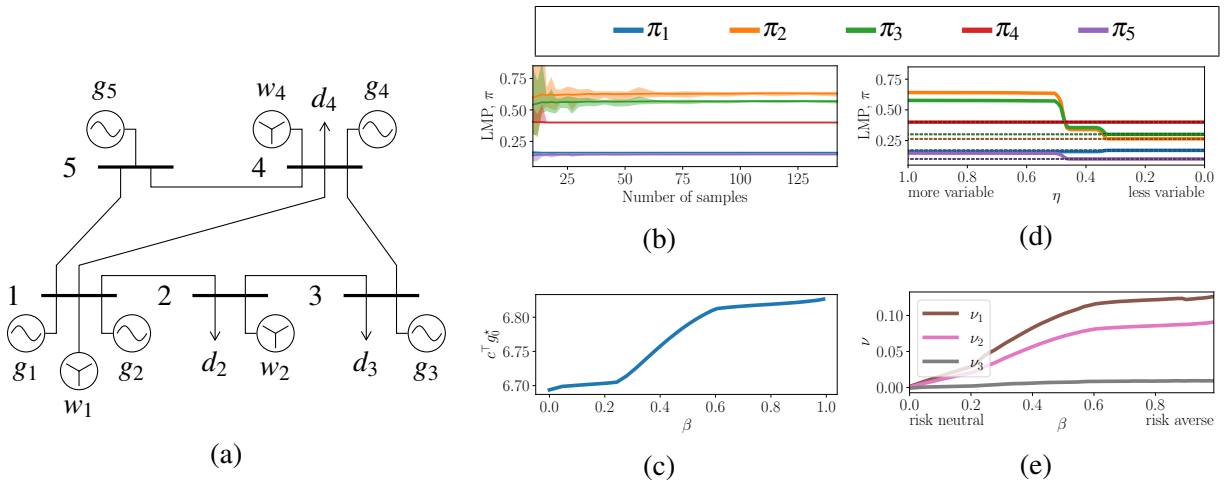

Figure 4.1: Evaluation of the prices for the 5-bus network in (a), depicting the (b) mean and range as a function of sample complexity with $\gamma = \beta = 0.9$, (c) nominal cost of generation as a function of β with $\gamma = 0.6$, (d) effect of scaling forecast error by η for $\gamma = \beta = 0.6$, where the dashed line shows the LMP of the nominal ED, and (e) reserve price, ν, as a function of β with $\gamma = 0.6$.

duality allows us to define electricity prices from this approximate problem. Specifically, let $\widehat{\lambda}_N, \widehat{\boldsymbol{\mu}}_N$ denote the dual multipliers for constraints (4.10b) and (4.10d), respectively.

Definition 2. *The vector of SAA-based risk-sensitive LMPs is defined as* $\widehat{\boldsymbol{\pi}}_N = \widehat{\lambda}_N^\star \mathbb{1} - \boldsymbol{H}^\intercal \widehat{\boldsymbol{\mu}}_N^\star$.

One can show that $\widehat{\boldsymbol{\pi}}_N \in \partial_{\boldsymbol{d}} \widehat{J}_N^\star(\boldsymbol{d})$, i.e., the SAA prices measure the sensitivity of the optimal cost of the SAA-based ED problem to the vector of nodal demands. Notice that since the N samples $\boldsymbol{\xi}^1, \ldots, \boldsymbol{\xi}^N$ are drawn randomly, the output of the SAA problem is itself random. Hence, the prices calculated from this sampled problem are random as well. Next, we study properties of these prices empirically.

4.4.1 Numerical experiments on a five-bus network example

We consider the heavily-loaded PJM 5-bus network from the IEEE PES Power Grid Library v17.08 [41]. The network, depicted in Figure 4.1a, is augmented with renewable generation at buses 1, 2, and 4, with 2.3, 1.5, and 0.9 per unit capacity, respectively. Wind outputs from three wind power plants from the New York area were used from NREL's synthetic dataset [27], treating the tuple of wind power outputs every 5 minutes over 2008-2011 as a single sample, $\boldsymbol{\xi}$.

The SAA approach is an effective mechanism for solving CVaR-sensitive ED, as Figure 4.1b reveals. The variance of the prices at each bus drops below 6×10^{-5} with just $N = 100$ samples, and below 3×10^{-6} with $N = 1000$ samples. With that in mind, all other simulations use 1000 samples.

The CVaR-sensitive dispatch presents a natural extension to its commonly studied deterministic variant. As Figure 4.1d shows, scaling the forecast error by η and taking $\eta \downarrow 0$ recovers the de-

terministic ED solution and the risk-sensitive LMPs reduce to conventional LMPs. Notice that nominal dispatch costs increase as the SO becomes more risk-averse in enforcing line limits (see Figure 4.1c). Regulation prices exhibit similar behavior with increased risk aversion, per Figure 4.1e. Hence, greater risk aversion to line limit violations results in dispatchable generators collecting more payment for reserve provision. Renewable suppliers, on the other hand, incur higher penalties for their impending uncertainty.

4.5 Revenue adequacy

The SO should ideally never run cash negative after settling all payments with market participants, i.e., the dispatch and pricing mechanism should be revenue adequate. In this section, we analyze when our risk-sensitive dispatch and pricing mechanism is revenue adequate. To that end, define the merchandising surplus (MS) as the aggregate payments received from consumers less the aggregate payments made to dispatchable and renewable suppliers:

$$\text{MS} = \boldsymbol{\pi}^{\mathsf{T}}(\boldsymbol{d} - \boldsymbol{g}_0^\star - \boldsymbol{\xi}_0) - \mathbb{1}^{\mathsf{T}}\boldsymbol{G}^\star\boldsymbol{\nu}^\star + \mathbb{1}^{\mathsf{T}}\boldsymbol{\nu}^\star = -\boldsymbol{\pi}^{\mathsf{T}}\boldsymbol{p}_0^\star,$$

where $\boldsymbol{p}_0^\star = \boldsymbol{g}_0^\star + \boldsymbol{\xi}_0 - \boldsymbol{d}$. We analyze conditions under which $\text{MS} \geq 0$ from the CVaR-based ED problem.

Proposition 5. *Suppose $\boldsymbol{X}^\star := (\boldsymbol{H} - \boldsymbol{H}\boldsymbol{G}^\star)\Delta\boldsymbol{\xi}$ has a smooth cumulative distribution function. Then, the merchandising surplus is given by*

$$MS = \boldsymbol{\mu}^{\star,\mathsf{T}}\boldsymbol{H}\boldsymbol{p}_0^\star = \boldsymbol{\mu}^{\star,\mathsf{T}}\big(\boldsymbol{f} - CVaR_\beta\left[\boldsymbol{X}^\star\right]\big). \tag{4.11}$$

$MS \geq 0$, if $f_i \geq CVaR_\beta[X_i^\star]$ for each $i = 1,\ldots,2\ell$ or $\boldsymbol{\mu}^\star = 0$.

Proposition 5 reveals that MS from our CVaR-sensitive ED problem arises due to congestion that results in price separation across different buses in the network. Without congestion in any scenario, $\boldsymbol{\mu}^\star = 0$, that implies $\text{MS} = 0$. Such a property is shared by MS obtained with LMPs from a deterministic ED problem. In fact, for a deterministic ED problem, MS equals the congestion rent $\boldsymbol{\mu}^{\star,\mathsf{T}}\boldsymbol{f}$. We recover that result by driving $\Delta\boldsymbol{\xi}$ to zero, that in turn makes $\boldsymbol{X}^\star$ identically zero making MS equal to $\boldsymbol{\mu}^{\star,\mathsf{T}}\boldsymbol{f}$ as is the case with conventional LMPs.

MS from our CVaR-sensitive ED problem can be viewed as the congestion rent with a modified line flow, $\boldsymbol{f} - \text{CVaR}_\beta\left[\boldsymbol{X}^\star\right]$. To gain more insights into the modifier, notice that $X_i^\star$ is composed of two terms: $\boldsymbol{H}_i\Delta\boldsymbol{\xi}$ and $\boldsymbol{H}_i(\boldsymbol{G}^\star\Delta\boldsymbol{\xi})$, where $\boldsymbol{H}_i$ denotes the i-th row of $\boldsymbol{H}$. The first term equals the induced flows on the i-th line due to nodal forecast errors $\Delta\boldsymbol{\xi}$. The second term equals the same from the dispatchable generator responses $\boldsymbol{G}^\star\Delta\boldsymbol{\xi}$ to said forecast errors. That is, $X_i^\star$ captures the net effect of forecast errors on the i-th line flow. The modifier satisfies

$$0 = \mathbb{E}[X_i^\star] \leq \text{CVaR}_\beta\left[X_i^\star\right] \leq \max X_i.$$

Thus, $\text{CVaR}_\beta\left[X_i^\star\right]$ increases from zero to $\max X_i$ as β ranges from zero to unity. While we cannot guarantee nonnegativity of MS for all problem instances, this range provides valuable insights into

when we might expect it. Specifically, when β is small (the SO is close to being risk neutral) or $\max X_i$ is smaller than f_i (when forecast errors are small or do not induce large enough net flows on the i-th line), we expect MS ≥ 0. It is encouraging that we obtained MS ≥ 1.14 for all our experiments on the five-bus network.

5. Conclusions and Future work

In this report, we studied the use of CVaR as a means of modeling risk of being unable to meet demand under various forms of uncertainty such as potential component failures and renewable supply.

In Chapter 2, we defined an alternative formulation of SCED that allows a system operator (SO) to trade-off between minimization of dispatch cost and reliability of power delivery, and explored its salient properties. We then proposed the critical region exploration (CRE) algorithm to solve it. In future studies, we aim to compare CRE with the popular Bender's decomposition technique on larger power networks for R-SCED, as proposed in [13, 42–45]. We also aim to extend our formulation and algorithm to model uncertainty in renewable power production.

In Chapter 3, we presented a risk-sensitive power procurement problem, where the risk refers to the inability of being able to provide adequate generation or satisfy line capacity limits. This risk is measured via conditional value at risk (CVaR). The risk parameters capture a SO's tolerance towards optimality and constraint violation. We then presented a sampling-based online stochastic primal-dual subgradient method for solving this problem, before illustrating our algorithm and formulation on a two-bus network example. The algorithm has high iteration complexity and runtime even for small risk-parameters–an aspect we aim to improve by exploiting structures such as smoothness of objective and constraint functions in the uncertain parameters. Our current work considers a specific way to model supply risk with uncertain renewable generation. The formulation of the market clearing problem can be altered to include procurement of reserve capacities and allowing for load sheds. We leave the consideration and comparison of various models of incorporating said risk for future work.

Finally in Chapter 4, we derived and analyzed prices from a CVaR-sensitive ED problem where transmission line flow constraints and generation limits are imposed in a risk-sensitive fashion. We showed that these prices have properties similar to LMPs derived from a deterministic ED problem. Approximations to these prices were derived using sample average approximation (SAA) that were empirically shown to asymptotically converge. Forward settlements and revenue adequacy issues were also analyzed. In the future, we are interested in addressing three areas of research in this direction. First, we aim to more fully analyze the implications of our proposed settlement scheme. For example, we want to understand if our proposed payments adequately incentivize generators to follow the SO-prescribed dispatch. In the event that they do not, we wish to study how risk parameters and wind variance affect aggregate side-payments necessary to incentivize the generators. Second, we want to study alternate risk models and their associated pricing mechanisms. That is, we want to understand other ways to encode and price supply risk than by defining risk-sensitive constraints on possible violations of line flow limits and generation capacities. Third, we hope to analytically establish the convergence properties, both with finitely many samples and in the asymptotic limit, of the SAA-based approximate prices. Besides these directions, our long-term goal is to incorporate unit commitment decisions and analyze CVaR-sensitive prices for day-ahead

market operations.

References

[1] O. Alsac and B. Stott, "Optimal load flow with steady-state security," *IEEE Transactions on Power Apparatus and Systems*, no. 3, pp. 745–751, 1974.

[2] A. Monticelli, M. Pereira, and S. Granville, "Security-constrained optimal power flow with post-contingency corrective rescheduling," *IEEE Transactions on Power Systems*, vol. 2, no. 1, pp. 175–180, 1987.

[3] F. Capitanescu and L. Wehenkel, "Improving the statement of the corrective security-constrained optimal power-flow problem," *IEEE Transactions on Power Systems*, vol. 22, no. 2, pp. 887–889, 2007.

[4] Z. Li, W. Wu, M. Shahidehpour, and B. Zhang, "Adaptive robust tie-line scheduling considering wind power uncertainty for interconnected power systems," *IEEE Transactions on Power Systems*, vol. 31, no. 4, pp. 2701–2713, 2016.

[5] F. Capitanescu, J. M. Ramos, P. Panciatici, D. Kirschen, A. M. Marcolini, L. Platbrood, and L. Wehenkel, "State-of-the-art, challenges, and future trends in security constrained optimal power flow," *Electric Power Systems Research*, vol. 81, no. 8, pp. 1731–1741, 2011.

[6] F. Bouffard and F. D. Galiana, "Stochastic security for operations planning with significant wind power generation," in *Power and Energy Society General Meeting-Conversion and Delivery of Electrical Energy in the 21st Century, 2008 IEEE*. IEEE, 2008, pp. 1–11.

[7] F. Capitanescu, M. Glavic, D. Ernst, and L. Wehenkel, "Contingency filtering techniques for preventive security-constrained optimal power flow," *IEEE Transactions on Power Systems*, vol. 22, no. 4, pp. 1690–1697, 2007.

[8] Y. Guo, S. Bose, and L. Tong, "On robust tie-line scheduling in multi-area power systems," *IEEE Transactions on Power Systems*, vol. 33, no. 4, pp. 4144–4154, 2017.

[9] A. N. Madavan, S. Bose, Y. Guo, and L. Tong, "Risk-sensitive security-constrained economic dispatch via critical region exploration," in *2019 IEEE Power Energy Society General Meeting (PESGM)*, 2019, pp. 1–5.

[10] O. Alsac, J. Bright, M. Prais, and B. Stott, "Further developments in lp-based optimal power flow," *IEEE Transactions on Power Systems*, vol. 5, no. 3, pp. 697–711, 1990.

[11] Y. C. Chen, A. D. Domínguez-García, and P. W. Sauer, "Measurement-based estimation of linear sensitivity distribution factors and applications," *IEEE Transactions on Power Systems*, vol. 29, no. 3, pp. 1372–1382, 2014.

[12] P. Renaud, *Transmission group procedure*, http://www.nyiso.com/public/webdocs/markets_operations/services/planning/Documents_and_Resources/FERC_Form_715_Filing/Planning_Reliability_Criteria/ngrid_transmission_planning_guide.pdf, National Grid USA Service Company, Inc., 2010.

[13] Y. Liu, M. C. Ferris, and F. Zhao, "Computational study of security constrained economic dispatch with multi-stage rescheduling," *IEEE Transactions on Power Systems*, vol. 30, no. 2, pp. 920–929, 2015.

[14] R. T. Rockafellar and S. Uryasev, "Conditional value-at-risk for general loss distributions," *Journal of banking & finance*, vol. 26, no. 7, pp. 1443–1471, 2002.

[15] F. Borrelli, A. Bemporad, and M. Morari, *Predictive control for linear and hybrid systems*. Cambridge University Press, 2017.

[16] T. I. P. T. F. on Benchmarks for Validation of Emerging Power System Algorithms, "Pglib optimal power flow benchmarks," https://github.com/power-grid-lib/pglib-opf, IEEE, 2018. [Online]. Available: https://github.com/power-grid-lib/pglib-opf

[17] T. Summers, J. Warrington, M. Morari, and J. Lygeros, "Stochastic optimal power flow based on conditional value at risk and distributional robustness," *International Journal of Electrical Power & Energy Systems*, vol. 72, pp. 116–125, 2015.

[18] A. N. Madavan and S. Bose, "A stochastic primal-dual method for optimization with conditional value at risk constraints," *Journal of Optimization Theory and Applications*, pp. 1–33, 2021.

[19] A. Charnes and W. W. Cooper, "Chance-constrained programming," *Management science*, vol. 6, no. 1, pp. 73–79, 1959.

[20] D. Bienstock, M. Chertkov, and S. Harnett, "Chance-constrained optimal power flow: Risk-aware network control under uncertainty," *Siam Review*, vol. 56, no. 3, pp. 461–495, 2014.

[21] L. Roald and G. Andersson, "Chance-constrained ac optimal power flow: Reformulations and efficient algorithms," *IEEE Transactions on Power Systems*, vol. 33, no. 3, pp. 2906–2918, 2017.

[22] E. Dall'Anese, K. Baker, and T. Summers, "Chance-constrained AC optimal power flow for distribution systems with renewables," *IEEE Transactions on Power Systems*, vol. 32, no. 5, pp. 3427–3438, 2017.

[23] M. Vrakopoulou, B. Li, and J. L. Mathieu, "Chance constrained reserve scheduling using uncertain controllable loads part i: Formulation and scenario-based analysis," *IEEE Transactions on Smart Grid*, vol. 10, no. 2, pp. 1608–1617, 2017.

[24] A. N. Madavan and S. Bose, "Risk-sensitive energy procurement with uncertain wind," in *2019 IEEE Global Conference on Signal and Information Processing (GlobalSIP)*, 2019, pp. 1–5.

[25] G. Calafiore and M. C. Campi, "Uncertain convex programs: randomized solutions and confidence levels," *Mathematical Programming*, vol. 102, no. 1, pp. 25–46, 2005.

[26] M. C. Campi and S. Garatti, "The exact feasibility of randomized solutions of uncertain convex programs," *SIAM Journal on Optimization*, vol. 19, no. 3, pp. 1211–1230, 2008.

[27] C. Draxl, A. Clifton, B.-M. Hodge, and J. McCaa, "The wind integration national dataset (wind) toolkit," *Applied Energy*, vol. 151, pp. 355–366, 2015.

[28] P. Pinson, "Wind energy: Forecasting challenges for its operational management," *Statist. Sci.*, vol. 28, no. 4, pp. 564–585, 11 2013. [Online]. Available: https://doi.org/10.1214/13-STS445

[29] Y. Dvorkin, "A chance-constrained stochastic electricity market," *IEEE Transactions on Power Systems*, vol. 35, no. 4, pp. 2993–3003, 2020.

[30] X. Kuang, Y. Dvorkin, A. J. Lamadrid, M. A. Ortega-Vazquez, and L. F. Zuluaga, "Pricing chance constraints in electricity markets," *IEEE Transactions on Power Systems*, vol. 33, no. 4, pp. 4634–4636, 2018.

[31] M. Lubin, Y. Dvorkin, and S. Backhaus, "A robust approach to chance constrained optimal power flow with renewable generation," *IEEE Transactions on Power Systems*, vol. 31, no. 5, pp. 3840–3849, 2016.

[32] A. Papavasiliou, S. S. Oren, and R. P. O'Neill, "Reserve requirements for wind power integration: A scenario-based stochastic programming framework," *IEEE Transactions on Power Systems*, vol. 26, no. 4, pp. 2197–2206, 2011.

[33] G. Pritchard, G. Zakeri, and A. Philpott, "A single-settlement, energy-only electric power market for unpredictable and intermittent participants," *Operations Research*, vol. 58, no. 4, pp. 1210–1219, 2010.

[34] J. M. Morales, A. J. Conejo, K. Liu, and J. Zhong, "Pricing electricity in pools with wind producers," *IEEE Transactions on Power Systems*, vol. 27, no. 3, pp. 1366–1376, 2012.

[35] S. Wong and J. D. Fuller, "Pricing energy and reserves using stochastic optimization in an alternative electricity market," *IEEE Transactions on Power Systems*, vol. 22, no. 2, pp. 631–638, 2007.

[36] R. T. Rockafellar, S. Uryasev *et al.*, "Optimization of conditional value-at-risk," *Journal of risk*, vol. 2, pp. 21–42, 2000.

[37] M. Ndrio, A. N. Madavan, and S. Bose, "Pricing conditional value at risk-sensitive economic dispatch," in *2021 IEEE Power Energy Society General Meeting (PESGM)*. IEEE, 2021, pp. 1–5.

[38] T. Summers, J. Warrington, M. Morari, and J. Lygeros, "Stochastic optimal power flow based on conditional value at risk and distributional robustness," *International Journal of Electrical Power And Energy Systems*, vol. 72, pp. 116–125, 2015, the Special Issue for 18th Power Systems Computation Conference.

[39] Y. Chen, Y. Wang, D. Kirschen, and B. Zhang, "Model-free renewable scenario generation using generative adversarial networks," *IEEE Transactions on Power Systems*, vol. 33, no. 3, pp. 3265–3275, 2018.

[40] E. Litvinov, "Design and operation of the locational marginal prices-based electricity markets," *IET Generation, Transmission Distribution*, vol. 4, no. 2, pp. 315–323, 2010.

[41] S. Babaeinejadsarookolaee, A. Birchfield, R. D. Christie, C. Coffrin, C. DeMarco, R. Diao, M. Ferris, S. Fliscounakis, S. Greene, R. Huang, C. Josz, R. Korab, B. Lesieutre, J. Maeght, D. K. Molzahn, T. J. Overbye, P. Panciatici, B. Park, J. Snodgrass, and R. Zimmerman, "The power grid library for benchmarking ac optimal power flow algorithms," 2019.

[42] T. Gomez, I. Perez-Arriaga, J. Lumbreras, and V. Parra, "A security-constrained decomposition approach to optimal reactive power planning," *IEEE Transactions on Power Systems*, vol. 6, no. 3, pp. 1069–1076, 1991.

[43] J. Martínez-Crespo, J. Usaola, and J. L. Fernández, "Security-constrained optimal generation scheduling in large-scale power systems," *IEEE Transactions on Power Systems*, vol. 21, no. 1, pp. 321–332, 2006.

[44] Y. Li and J. D. McCalley, "Decomposed scopf for improving efficiency," *IEEE Transactions on Power Systems*, vol. 24, no. 1, pp. 494–495, 2009.

[45] D. Phan and J. Kalagnanam, "Some efficient optimization methods for solving the security-constrained optimal power flow problem," *IEEE Transactions on Power Systems*, vol. 29, no. 2, pp. 863–872, 2014.